Molecular Microbiology (2015) 96(3), 526–547
doi:10.1111/mmi.12954
First published online 26 February 2015

The Crc protein participates in down-regulation of the Lon gene to promote rhamnolipid production and *rhl* quorum sensing in *Pseudomonas aeruginosa*

Nana Yang,[1] Shuting Ding,[1,2] Feifei Chen,[1] Xue Zhang,[1] Yongjie Xia,[1] Hongxia Di,[1] Qiao Cao,[1] Xin Deng,[3] Min Wu,[4] Catherine C.L. Wong,[5] Xiao-Xu Tian,[5] Cai-Guang Yang,[1] Jing Zhao[2] and Lefu Lan[1]*

[1]*Shanghai Institute of Materia Medica, Chinese Academy of Sciences, 555 Zuchongzhi Road, Pudong Zhangjiang Hi-Tech Park, Shanghai 201203, China.*
[2]*Institute of Chemistry and BioMedical Sciences, State Key Laboratory of Pharmaceutical Biotechnology, School of Life Sciences, Nanjing University, Nanjing 210093, China.*
[3]*Department of Chemistry and Institute for Biophysical Dynamics, The University of Chicago, Chicago, IL 60637, USA.*
[4]*Department of Basic Sciences, University of North Dakota School of Medicine and Health Sciences, Grand Forks, ND 58203, USA.*
[5]*Mass Spectrometry Division, National Center for Protein Science Shanghai, Shanghai Institute of Biochemistry and Cell Biology, Chinese Academy of Science, 333 Haike Road, Shanghai 201210, China.*

Summary

Rhamnolipid acts as a virulence factor during *Pseudomonas aeruginosa* infection. Here, we show that deletion of the catabolite repression control (*crc*) gene in *P. aeruginosa* leads to a rhamnolipid-negative phenotype. This effect is mediated by the down-regulation of *rhl* quorum sensing (QS). We discover that a disruption of the gene encoding the Lon protease entirely offsets the effect of *crc* deletion on the production of both rhamnolipid and *rhl* QS signal C4-HSL. Crc is unable to bind *lon* mRNA *in vitro* in the absence of the RNA chaperon Hfq, while Crc contributes to Hfq-mediated repression of the *lon* gene expression at a posttranscriptional level. Deletion of *crc*, which results in up-regulation of *lon*, significantly reduces the *in vivo* stability and abundance of the RhlI protein that synthesizes C4-HSL, causing the attenuation of *rhl* QS. Lon is also capable of degrading the RhlI protein *in vitro*. In addition, constitutive expression of *rhlI* suppresses the defects of the *crc* deletion mutant in rhamnolipid, C4-HSL and virulence on lettuce leaves. This study therefore uncovers a novel posttranscriptional regulatory cascade, Crc-Hfq/Lon/RhlI, for the regulation of rhamnolipid production and *rhl* QS in *P. aeruginosa*.

Accepted 28 January, 2015. *For correspondence. E-mail llan@simm.ac.cn; Tel. (+86) 21 5080 3109; Fax (+86) 21 5080 7088.

Introduction

Pseudomonas aeruginosa is one of the most dreaded Gram-negative bacteria in hospital settings (Stover *et al.*, 2000; National Nosocomial Infections Surveillance, 2004). Notably, *P. aeruginosa* is the leading cause of morbidity and mortality in patients with cystic fibrosis (Lyczak *et al.*, 2002). As an opportunistic pathogen, this bacterium owes its success to its nutritional versatility, its antibiotic resistance, its propensity to form biofilms and its ability to produce a large arsenal of virulence factors that interfere with host defenses (Jimenez *et al.*, 2012; Balasubramanian *et al.*, 2013).

Rhamnolipid produced by *P. aeruginosa* is a virulence determinant in lung infections (Zulianello *et al.*, 2006). Rhamnolipid is able to kill polymorphonuclear leukocytes (Jensen *et al.*, 2007) and macrophages (McClure and Schiller, 1996), and may thus contribute to the establishment and maintenance of infection (Rumbaugh *et al.*, 1999). Moreover, rhamnolipid is reported to affect several key virulence-associated traits of *P. aeruginosa*, including bacterial cell motility and biofilm development (Caiazza *et al.*, 2005). In *P. aeruginosa*, rhamnolipid is a class of glycolipids produced by three sequential reactions mediated by RhlA, RhlB and RhlC (Reis *et al.*, 2011). Besides acting as a virulence factor in the human host, rhamnolipids are also produced outside of the host and show outstanding potential as commercial biosurfactants, thanks to their unique chemical characteristics (Reis *et al.*, 2011).

In *P. aeruginosa*, the *rhlA* and *rhlB* genes are arranged as an operon (*rhlAB*) (Reis *et al.*, 2011). Like *rhlAB*, *rhlC* is also controlled by the *rhl* quorum sensing (QS) system (Rahim *et al.*, 2001), a key regulator of the pathogenesis of *P. aeruginosa*, by coordinating cell density-dependent processes like virulence factor expression (Schuster and Greenberg, 2006; Williams and Camara, 2009; Rutherford and Bassler, 2012; O'Loughlin *et al.*, 2013). The *rhl* QS system, a subordinate to the *las* QS system, consists of RhlR, RhlI and the signal molecule N-butyryl-L-homoserine lactone (C4-HSL) (Schuster and Greenberg, 2006; Rutherford and Bassler, 2012). RhlR acts as an activator of the *rhlAB* operon, *rhlC* and *rhlI*, after forming a complex with C4-HSL, which is synthesized by RhlI (Schuster and Greenberg, 2006; Rutherford and Bassler, 2012). Moreover, a group of regulators related to the QS systems has been identified and reported to either directly or indirectly influence the production of rhamnolipid (Reis *et al.*, 2011; Cao *et al.*, 2014). Recently, it has been reported that the expression of *rhlA* can also be positively regulated at the posttranscriptional level by the non-coding RNA NrsZ (Wenner *et al.*, 2013). Therefore, the regulation of rhamnolipid production is more complex than previously thought.

Here, we show that the catabolite repression control (Crc) protein is involved in rhamnolipid production in *P. aeruginosa*. We found that Crc exerts its role on rhamnolipid production by activating *rhl* QS, via the down-regulation of Lon protease. We further demonstrated that Lon degrades the RhlI protein *in vivo* and *in vitro*. In addition, we showed that Crc contributes to Hfq-mediated repression of Lon expression at a posttranscriptional level.

Results

High-throughput screening of genes required for rhamnolipid production in P. aeruginosa *identifies crc*

To identify genetic factors that govern rhamnolipid production in *P. aeruginosa*, we performed a screen for rhamnolipid defective mutants using a library of PAO1::*rhlA*-*lacZ* (Supporting Information Table S1) transposon mutants and a methylene blue/cetyltrimethylammonium bromide (CTAB) agar plate method (Kohler *et al.*, 2000; Gupta *et al.*, 2009; Cao *et al.*, 2014). Approximately 50 000 transposon insertion mutants were visually analyzed by scoring the severe decrease in the size of the blue halo surrounding the bacterial colonies on the CTAB agar plates, which indicates the production of rhamnolipid (Kohler *et al.*, 2000; Gupta *et al.*, 2009). Sixty-two mutants were initially chosen. The precise insertion site of the transposon was subsequently determined for these mutants, 45 of which were unique (Supporting Information Table S3). These transposon insertion mutations mapped to 14 genes and 5 intergenic regions (Supporting Information Table S3). Among those we found, several were already known to be essential for the synthesis of rhamnolipids in *P. aeruginosa*. These were *rhlA*, *rhlB* and *rhlR* (Supporting Information Table S3, Fig. S1). The transposon disruption of *bioF*, *apaH*, *aroP2*, *cysH*, *relA*, *PA2852*, *PA4852*, *tufA*, *gltB*, *ntrB* or the *crc* genes resulted in a rhamnolipid-negative phenotype (Supporting Information Fig. S1). We therefore hypothesized that some of these genes might play a critical role in the control of rhamnolipid production in *P. aeruginosa*. In this study, we chose *crc* for further characterization because it is involved in carbon catabolite repression (CCR) (Gorke and Stulke, 2008; Rojo, 2010), which could provide a link between nutritional cues and rhamnolipid production (Caiazza *et al.*, 2005) (Supporting Information Table S3, Fig. S1).

To further confirm the role of Crc in the control of rhamnolipid biosynthesis, we generated a *crc* null mutant strain (Δ*crc*, Supporting Information Table S1) as described in the *Experimental procedures* section and we examined its phenotype on a CTAB agar plate. As shown in Fig. 1A, the Δ*crc* strain, like the *crc* gene transposon insertion mutant (Supporting Information Fig. S1), was defective in the production of rhamnolipid. Quantitative analysis of rhamnolipid indicated that the deletion of the *crc* gene resulted in an approximately 95% decrease in rhamnolipid production (Fig. 1B). Furthermore, introduction of a wild-type *crc* gene (p-*crc*, Supporting Information Table S1) into the Δ*crc* strain fully restored rhamnolipid production to the level of wild-type PAO1 (Fig. 1A and B). Based on these results, we concluded that Crc is a positive regulator of rhamnolipid production in *P. aeruginosa*.

Transcriptome analysis of genes regulated by Crc

To assess the impact of Crc on global gene expression and the expression of genes related to rhamnolipid biosynthesis in *P. aeruginosa*, we performed a transcriptome analysis of wild-type PAO1 and its *crc* deletion mutant (Δ*crc*) using RNA-seq when bacteria were grown in M8 minimal medium for 9 h. The M8 minimal medium shares similar components with CTAB agar medium that was used to screen for rhamnolipid defective mutants (Supporting Information Fig. S1), except for methylene blue, CTAB and agar. As shown in Supporting Information Table S4, the transcripts of 69 genes were down-regulated by *crc* deletion while 72 were up-regulated at least twofold (cutoff limitation for fold change ≥ 2 or ≤ 0.5 and Cuffdiff P-value < 0.05 was used to select differential expression genes). The affected 141 genes belong to several functional categories, primarily metabolism, transcriptional regulation, transport of small molecules and hypothetical protein (Supporting Information Table S4). These results indicate that Crc has a profound impact on global gene expression in *P. aeruginosa*.

One observation of note is that the transcripts of *rhlA* and *rhlB* were decreased by approximately 75% and 83% in the Δ*crc* strain compared with that of the wild-type PAO1 strain

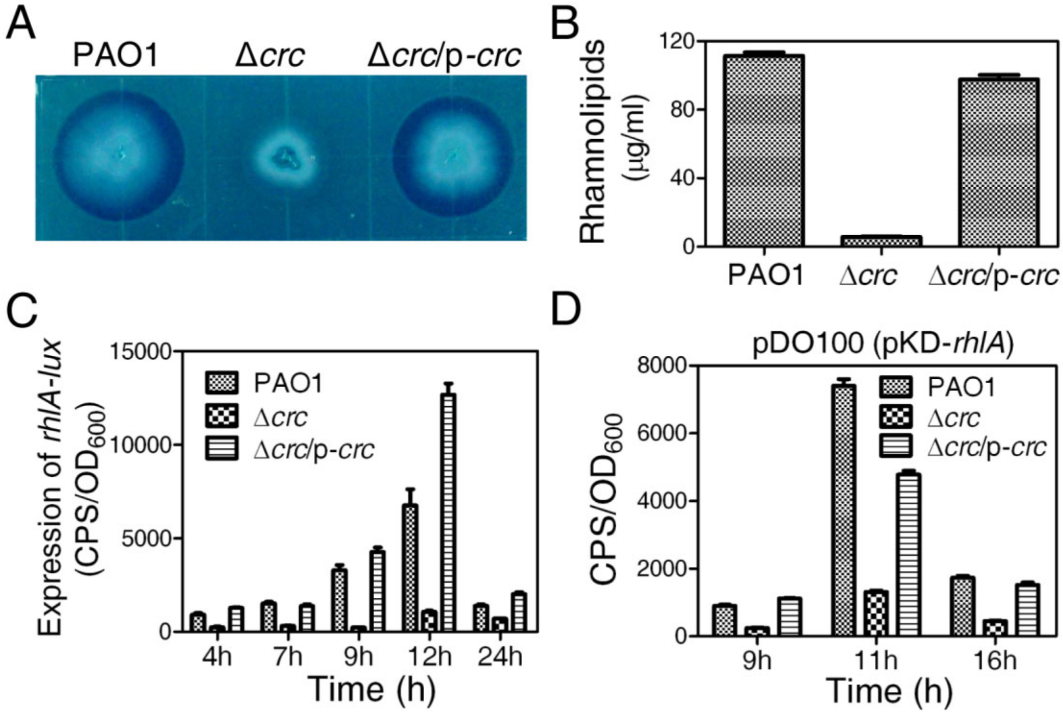

Fig. 1. Effect of *crc* deletion on rhamnolipid production, *rhlA* promoter activity and C4-HSL content. In all panels, PAO1 and Δ*crc* harbor plasmid PAK1900 respectively.
A. Bacterial strains were inoculated onto a CTAB plate and incubated at 37°C for 24 h and then for 48 h at room temperature. The presence of a blue halo surrounding the colonies indicates the production of rhamnolipids.
B. The amount of rhamnolipids in culture supernatants of *Pseudomonas aeruginosa* was determined by an indirect assay (orcinol test).
C. Expression of *rhlA-lux* in PAO1 and its derivatives was measured at different time points during bacteria growth in M8 minimal medium.
D. Relative amounts of C4-HSL measured by the pDO100 (pKD-*rhlA*) system. PAO1 and its derivatives were grown in M8 minimal medium at 37°C for 9 h with shaking (250 r.p.m.), showing comparable growth behavior (data not shown). The supernatants of tested strains were subsequently prepared and measured for their ability to promote the luminescence values of the C4-HSL reporter strain pDO100 (pKD-*rhlA*) at different time points after the addition of a tested sample, as indicated. CPS values became an indirect measure of supernatant C4-HSL.
Values represent means ± standard error of the mean (SEM) and each value was performed with triplicate biological replicates.

(Supporting Information Table S4) respectively. We also observed that the transcripts of *rhlC* were decreased by approximately 56% with a Cuffdiff *P*-value of 0.098 (Supporting Information Table S5). The *rhlA*, *rhlB* and *rhlC* are important for rhamnolipid biosynthesis (Ochsner *et al*., 1994; Ochsner and Reiser, 1995). Therefore, it is likely that the decreased abundance of these mRNAs may be responsible for the decreased rhamnolipid production of the Δ*crc* strain (Fig. 1A and B). In order to verify the RNA-seq results of *rhlAB* and *rhlC* expression, *rhlA* and *rhlC* were subjected to quantitative real-time polymerase chain reaction (qRT-PCR) analysis. As shown in Supporting Information Table S5, the qRT-PCR analysis showed similar results to those of RNA-seq analysis.

Next, we asked whether decreased *rhlA* promoter activity causes the reduced abundance of *rhlAB* mRNA. In order to assess this possibility, we measured the activities of an *rhlA* promoter-*lux* fusion (*rhlA-lux*) (Cao *et al*., 2014) in a wild-type PAO1 strain, a *crc* deletion strain (Δ*crc*) and in strain PAO1Δ*crc*(p-*crc*) complemented with a plasmid-borne copy of *crc* respectively. The expression of the *rhlA-lux* fusion in Δ*crc* was significantly lower than that of the other strains when bacteria were grown in M8 minimal medium (Fig. 1C). For instance, the expression of *rhlA-lux* in Δ*crc* was only 7% of that found in the wild-type PAO1 strain when bacteria were grown in M8 minimal medium for 9 h, a culture condition for RNA preparation used for RNA-seq analysis and qRT-PCR analysis. The decrease in the expression of *rhlA-lux* caused by *crc* disruption was suppressed by reintroducing a wild-type *crc* gene (Fig. 1C). Thus, the reduced transcripts of *rhlAB* in the Δ*crc* strain (Supporting Information Tables S4 and S5) are likely a result of decreased *rhlAB* promoter activity (Fig. 1C).

Because RhlR acts as an activator of the *rhlAB* operon after being complexed to C4-HSL, which is synthesized by RhlI (Schuster and Greenberg, 2006; Rutherford and Bassler, 2012), we therefore tested whether Crc could affect the transcript abundance of *rhlR* and *rhlI* using qRT-PCR analysis. Consistent with the RNA-seq data, qRT-PCR results showed that the *crc* deletion exhibited

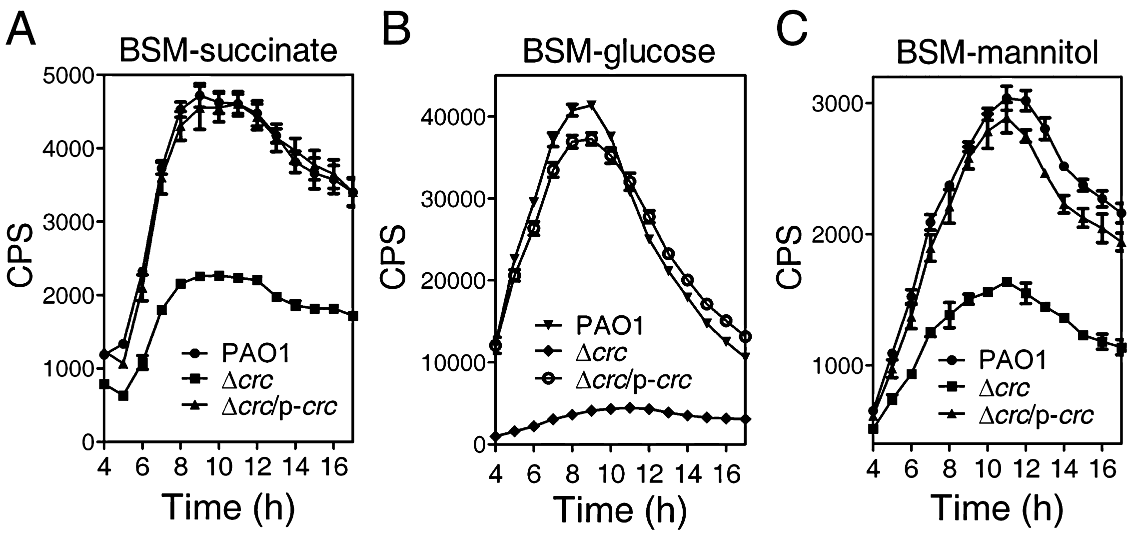

Fig. 2. Effect of *crc* deletion on *rhl* QS when bacteria were cultivated under different carbon sources. In all panels, PAO1 and Δ*crc* harbor plasmid PAK1900 respectively. The relative amounts of C4-HSL were measured using pDO100 (pKD-*rhlA*) system when PAO1 and its derivatives were grown in BSM medium amended with succinate (A), glucose (B) or mannitol (C) at 37°C for 9 h with shaking (250 r.p.m.). PAO1 and its derivatives showed comparable growth behavior (data not shown). All results were normalized to OD_{600}. Values represent means ± standard error of the mean (SEM) and each value was performed with triplicate biological replicates. The assays were independently repeated at least three times with similar results obtained, and the graphs show a set of representative data.

only a small effect on the mRNA expression of either *rhlR* or *rhlI*. As shown in Supporting Information Table S5, deletion of *crc* reduced the transcripts of *rhlR* and *rhlI* by 41% and 33% respectively.

Deletion of the crc *gene compromises the production of the rhl QS signal C4-HSL*

As aforementioned, deletion of the *crc* gene caused substantially reduced expression of *rhlAB* (Supporting Information Tables S4 and S5, and Fig. 1C). Given that the expression of *rhlAB* is controlled by the *rhl* QS system (Brint and Ohman, 1995; Ochsner and Reiser, 1995), we next sought to determine whether the *crc* deletion alters the level of the *rhl* QS signal C4-HSL content. We measured the content of the RhlI-dependent autoinducer C4-HSL in a wild-type PAO1 strain, a Δ*crc* strain and a complementary strain (Δ*crc*/p-*crc*) when bacteria were grown in M8 minimal medium, using the pDO100 (pKD-*rhlA*) system (Supporting Information Table S1) that carries a *lux* reporter fused with an *rhlA* promoter (Liang *et al.*, 2011; Cao *et al.*, 2014). We observed that the supernatants prepared from either the wild-type PAO1 strain or the complemented strain (Δ*crc*/p-*crc*), but not the Δ*crc* strain, markedly promoted luminescence values (Fig. 1D), and thereby C4-HSL levels (Liang *et al.*, 2011).

As Crc together with Hfq regulates CCR in *Pseudomonas* (Madhushani *et al.*, 2014; Sonnleitner and Blasi, 2014), we next sought to determine the effect of Crc on the content of C4-HSL when *P. aeruginosa* was cultivated under different carbon sources. We grew the bacteria in basal salt medium (BSM) supplemented with succinate (a preferred carbon source), glucose (an intermediate carbon source) or mannitol (a poor carbon source) as the sole carbon source (Sonnleitner *et al.*, 2009), and measured the relative C4-HSL levels using the pDO100 (pKD-*rhlA*) system as described above. When the C4-HSL reporter strain pDO100 was treated with the supernatants prepared from the Δ*crc* strain grown in BSM medium supplemented with succinate (Fig. 2A), glucose (Fig. 2B) and mannitol (Fig. 2C), the maximum expression of *rhlA-lux* was about 46% (Fig. 2A), 10% (Fig. 2B) and 55% (Fig. 2C) of that found in the wild-type PAO1 strain respectively. The introduction of a wild-type *crc* gene into the Δ*crc* strain could fully suppress the defect of the Δ*crc* strain in C4-HSL production (Fig. 2A–C), suggesting that Crc was stimulating C4-HSL production in *P. aeruginosa*. Additionally, these observations also suggest that the strength of the regulatory effect of Crc on C4-HSL production might occur in a carbon source-dependent manner (Fig. 2). However, this hypothesis awaits further investigations. Nonetheless, these results indicate that the deletion of the *crc* gene compromises the production of the *rhl* QS signal C4-HSL.

A genome-wide screen for suppressors of the crc deletion identifies mutations in lon *and* clpx

Crc was shown to negatively affect the expression of some genes at a posttranscriptional level (Gorke and Stulke, 2008; Sonnleitner *et al.*, 2009; Rojo, 2010; Madhushani

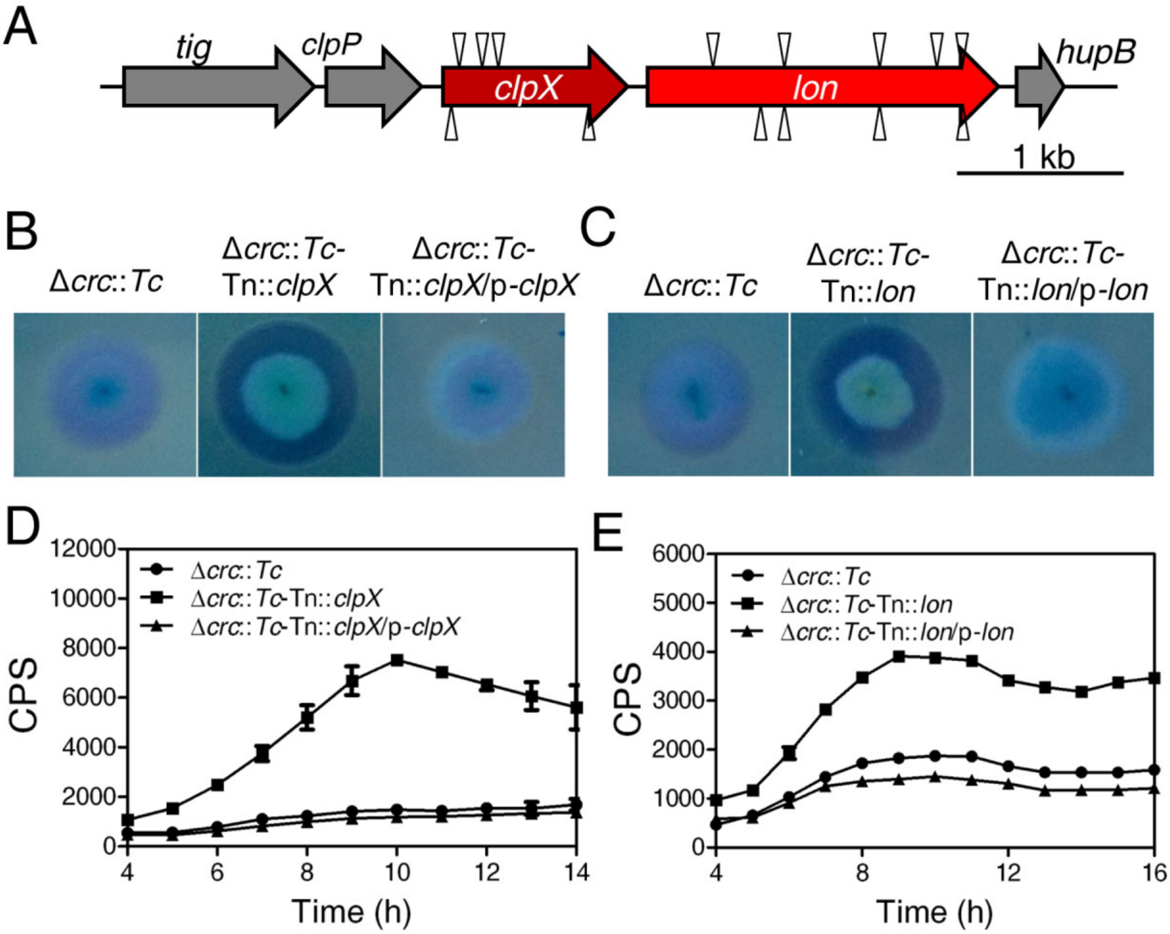

Fig. 3. Disruption of either *clpX* or *lon* suppresses the effect of *crc* deletion on the production of rhamnolipid and C4-HSL. In all panels, Δ*crc*::*Tc* strain (*crc* gene deletion, Supporting Information Table S1), Δ*crc*::*Tc*-Tn::*clpX* (Δ*crc*::*Tc* strain with a transposon insertion in *clpX*, Supporting Information Table S6) and Δ*crc*::*Tc*-Tn::*lon* (Δ*crc*::*Tc* strain with a transposon insertion in *lon*, Supporting Information Table S6) harbor plasmid PAK1900 respectively.
A. Schematic representation of *clpX* and *lon* genes, and the transposon insertion site (indicated by the triangle).
B. Effect of *clpX* disruption on the rhamnolipid production by Δ*crc*::*Tc* strain.
C. Effect of *lon* disruption on the rhamnolipid production by Δ*crc*::*Tc* strain. In B and C, bacterial strains were inoculated onto a CTAB plate and incubated at 37°C for 24 h and then for 48 h at room temperature.
D. Effect of *clpX* disruption on the production of C4-HSL by Δ*crc*::*Tc* strain.
E. Effect of *lon* disruption on the production of C4-HSL by Δ*crc*::*Tc* strain. In D and E, bacteria were grown in M8 minimal medium at 37°C for 9 h with shaking (250 r.p.m.) and then the supernatants were subsequently prepared and measured for their relative C4-HSL contents using pDO100 (pKD-*rhlA*) system. All results were normalized to OD_{600}. Values represent means ± standard error of the mean (SEM) and each value was performed with triplicate biological replicates.

et al., 2014; Sonnleitner and Blasi, 2014). Thus, we reasoned that the absence of Crc should result in the increased expression of some proteins, which in turn might contribute to the attenuation of rhamnolipid and C4-HSL production in *P. aeruginosa*. To test this hypothesis, we performed a suppressor screen using a library of Δ*crc*::*Tc* transposon insertion mutants and a phenotypic assay in order to assess rhamnolipid production on CTAB agar plates. The Δ*crc*::*Tc* strain is a *crc* deletion mutant (Supporting Information Table S1), whose *crc* gene is replaced by a tetracycline resistance gene and therefore the gentamicin resistance cassette of the transposon can be used as a selectable marker. We screened approximately 55 000 mutants (10 × genome coverage) on CTAB agar plates and identified 18 unique suppressor mutants with wild-type or near wild-type levels of rhamnolipid production (Supporting Information Table S6, Fig. S2A). Among the 18 suppressor mutants, half of them showed insertions in different regions of *lon*, a gene encoding the adenosine triphosphate (ATP)-dependent protease Lon, while 5 had insertions in the *clpX* gene (Supporting Information Table S6 and Fig. 3A) that encodes an alternative ATP-binding subunit of ATP-dependent Clp protease. The other four identified targets included *PA1335* (encoding a two-component response regulator), *pstA* (encoding a phosphate ABC transporter membrane protein) and two additional genes (*PA0146* and *PA2458*) with as yet unknown functions (Supporting Information Table S6).

As the disruption of Crc reduces the level of the *rhl* QS signal C4-HSL (Figs 1D and 2), we next examined whether the transposon insertion in these six genes could each alleviate this effect. As shown in Supporting Information Fig. S2B, the *lon*, *clpX* and *PA2458* insertions led to dramatically increased C4-HSL content when compared with its parent strain Δ*crc*::*Tc*. However, the transposon insertion in the *PA0146*, *PA1335* or *pstA* genes had no significant impact on the production of C4-HSL by the Δ*crc*::*Tc* strain (Supporting Information Fig. S2B). Given that the regulatory effect of Crc on rhamnolipid production was likely mediated through the *rhl* QS (Figs 1 and 2), we choose the *lon*, *clpX* and *PA2458* transposon insertion mutants for further characterization. To exclude the possibility of an artifact of transposition, we performed complementation analysis on these three selected mutants. As shown in Supporting Information Fig. S3, the introduction of a wild-type *PA2458* gene into the Δ*crc*::*Tc*-Tn::*PA2458* (additional disruption of *PA2458* gene by transposon insertion in the Δ*crc*::*Tc* strain) cannot fully restore the production of either rhamnolipid (Supporting Information Fig. S3A) or C4-HSL (Supporting Information Fig. S3B) to the levels of the Δ*crc*::*Tc* strain. Ectopic expression of the *clpX* gene in strain Δ*crc*::*Tc*-Tn::*clpX* resulted in reduced levels of rhamnolipid (Fig. 3B) and C4-HSL (Fig. 3D) as observed for Δ*crc*::*Tc*. A similar phenomenon was also observed in the case of the complementation test against the Δ*crc*::*Tc*-Tn::*lon* mutant (Fig. 3C and E).

In the *P. aeruginosa* chromosome, *lon* is immediately downstream of *clpX* (Stover *et al*., 2000) (Fig. 3A). To verify that the effects of Δ*crc*::*Tc*-Tn::*lon* were due to the *lon* disruption and not a polar effect, we generated a *lon* deletion in the Δ*crc* strain. The resulting mutant, termed Δ*crc*Δ*lon* (Supporting Information Table S1), was phenotypically similar to the Δ*crc*::*Tc*-Tn::*lon* mutant with respect to wild-type levels of rhamnolipid (Supporting Information Fig. S4A) and C4-HSL production (Supporting Information Fig. S4B). Ectopic expression of the *lon* gene in strain Δ*crc*Δ*lon* resulted in reduced levels of rhamnolipid and C4-HSL as observed for Δ*crc* (Supporting Information Fig. S4). These data strongly indicate that the inactivation of *lon* can abolish the effects of *crc* deletion on the production of C4-HSL and rhamnolipid in *P. aeruginosa*.

Lon and ClpX are negative regulators of rhl *QS*

To further investigate the role of *lon* and *clpX* in the regulation of *rhl* QS, we created a *lon* gene deletion mutant (Δ*lon*) (Supporting Information Table S1) and a *clpX* gene deletion mutant (Δ*clpX*) (Supporting Information Table S1) in the wild-type PAO1 background respectively. As expected, the absence of either *lon* or *clpX* caused an increase in rhamnolipid production (Fig. 4A). We further observed that constitutive expression of either *lon* or *clpX* significantly suppressed the production of rhamnolipid (Fig. 4B) and C4-HSL (Fig. 4C) by the wild-type PAO1. As shown in Fig. 4B, both PAO1/p-*lon-F* strain (Supporting Information Table S1) and the PAO1/p-*clpX* strain displayed more than 50% less rhamnolipid production than wild-type PAO1 (harboring PAK1900). Similarly, introduction of p-*lon-F* or p-*clpX* (Supporting Information Table S1) significantly ($P < 0.05$) reduced the *rhl* signal C4-HSL content of the wild-type PAO1 strain, by 62% and 40%, respectively, as estimated by the maximum expression of *rhlA-lux* in the C4-HSL reporter strain pDO100 (Fig. 4C). These results further suggested that Lon and ClpX represent negative regulators of *rhl* QS in *P. aeruginosa*. Moreover, either the constitutive expression of *lon* in the Δ*clpX* strain or the constitutive expression of *clpX* in the Δ*lon* strain significantly decreased the C4-HSL content by more than 80% (Fig. 4D and E), indicating that Lon modulates the *rhl* QS independently of ClpX, and vice versa. Taken together, these results suggest that components of the protein quality control (PQC) system (Gottesman, 1996; Gottesman *et al*., 1997; Wickner *et al*., 1999), especially Lon and ClpX, play a negative role in the regulation of *rhl* QS in *P. aeruginosa*. Given that constitutive expression of *lon* has a more pronounced negative effect on the C4-HSL content than that of *clpX* (Fig. 4C–E), we decided to focus on the role of Lon in this study.

Crc inhibits the expression of lon *at a posttranscriptional level*

As a protease, Lon may take part in the negative regulation of *rhl* QS by degrading quorum-sensing proteins such as autoinducer synthesis protein LasI (Takaya *et al*., 2008) and RhlI. That inactivation of *lon* totally suppresses the effect of *crc* deletion on *rhl* QS (Fig. 3C and E and Supporting Information Fig. S4) and that Lon is a negative regulator of *rhl* QS (Fig. 4) prompted us to examine whether Crc can inhibit the expression of *lon*. To this end, we constructed a transcriptional *lacZ* fusion (*lon-lacZ*, Supporting Information Table S1) and a translational fusion (*lon'-'lacZ*, Supporting Information Table S1) to the *lon* promoter and then measured the expression of β-galactosidase in a wild-type PAO1 strain and in a *crc* deletion mutant strain (Δ*crc*) respectively. As shown in Fig. 5A, the expression of the transcriptional *lon-lacZ* fusion was not significantly affected by the deletion of the *crc* gene. However, synthesis of the Lon-LacZ fusion protein was increased (> 0.8-fold) in the Δ*crc* strain when compared with that of wild-type PAO1 (Fig. 5B). In addition, providing a wild-type *crc* gene suppressed the increase in

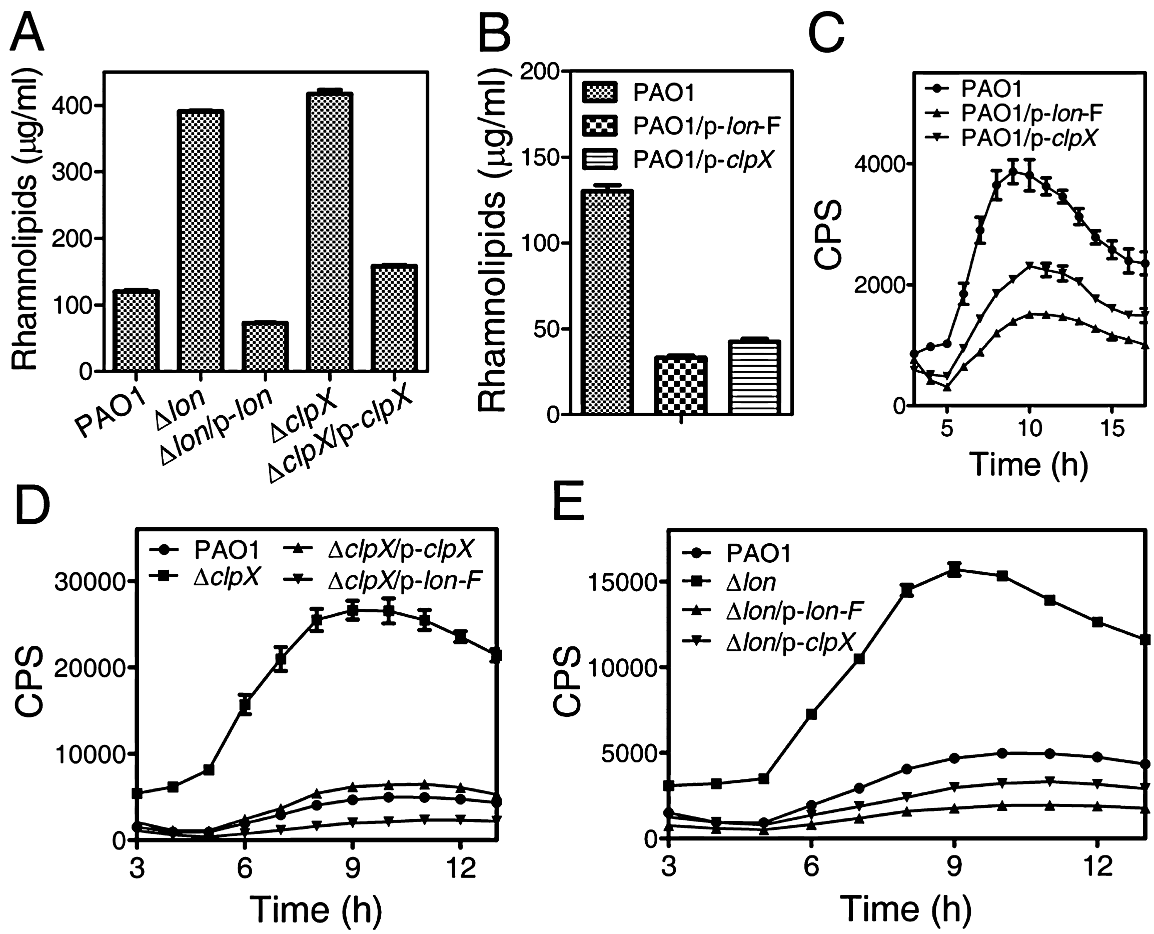

Fig. 4. ClpX and Lon are negative regulators of *rhl* QS. In all panels, PAO1, Δ*clpX* and Δ*lon* harbor plasmid PAK1900 respectively.
A and B. The amounts of rhamnolipids in culture supernatants of *Pseudomonas aeruginosa* were determined by an indirect assay (orcinol test). Bacteria were grown in M8 minimal medium at 37°C for 48 h with shaking (250 r.p.m.).
C. Effect of constitutive expression of either *clpX* or *lon* on the production of C4-HSL in wild-type PAO1 strain.
D. Effect of constitutive expression of either *clpX* or *lon* on the production of C4-HSL in a *clpX* deletion mutant strain (Δ*clpX*).
E. Effect of constitutive expression of either *clpX* or *lon* on the production of C4-HSL in a *lon* deletion mutant strain (Δ*lon*). In C, D and E, relative amount of C4-HSL measured by the pDO100 (pKD-*rhlA*) system when bacteria were grown in M8 minimal medium at 37°C for 9 h with shaking (250 r.p.m.). All results were normalized to OD_{600}. Values represent means ± standard error of the mean (SEM) and each value was performed with triplicate biological replicates.

lon'-'lacZ expression caused by the *crc* deletion (Fig. 5B). To further examine the effect of the *crc* deletion on the transcript level of *lon*, qRT-PCR analysis was performed on steady-state mRNA samples from wild-type PAO1 and Δ*crc* strain when bacteria were grown in an M8 minimal medium for 9 h. In agreement with the results of RNA-seq and transcriptional reporter fusion (*lon-lacZ*), we observed no significant difference in *lon* mRNA abundance between wild-type PAO1 and Δ*crc* strain (Supporting Information Table S5). These results indicate that the expression of *lon* is negatively controlled by Crc at a posttranscriptional level.

To further confirm that Crc negatively modulates the expression of *lon* at a posttranscriptional level, we constructed an integration vector mini-ctx-*lon-flag* (Supporting Information Table S1) and measured the expression of Lon-flag in a PAO1 strain (PAO1::*lon-flag*), a Δ*crc* strain (Δ*crc*::*lon-flag*) and a complementary strain (Δ*crc*::*lon-flag*/p-*crc*) by Western blot analysis using anti-FLAG antibodies. As shown in Fig. 5C, Δ*crc*::*lon-flag* strain exhibited a 60% increase in the expression of Lon-flag compared with its parent strain (PAO1::*lon-flag*), whereas the introduction of a plasmid carrying a wild-type *crc* gene (p-*crc*) (p-*crc*, Supporting Information Table S1) significantly decreased the expression of Lon-flag in the Δ*crc*::*lon-flag* strain by approximately 65%, suggesting that Crc inhibits the expression of *lon* at a posttranscriptional level.

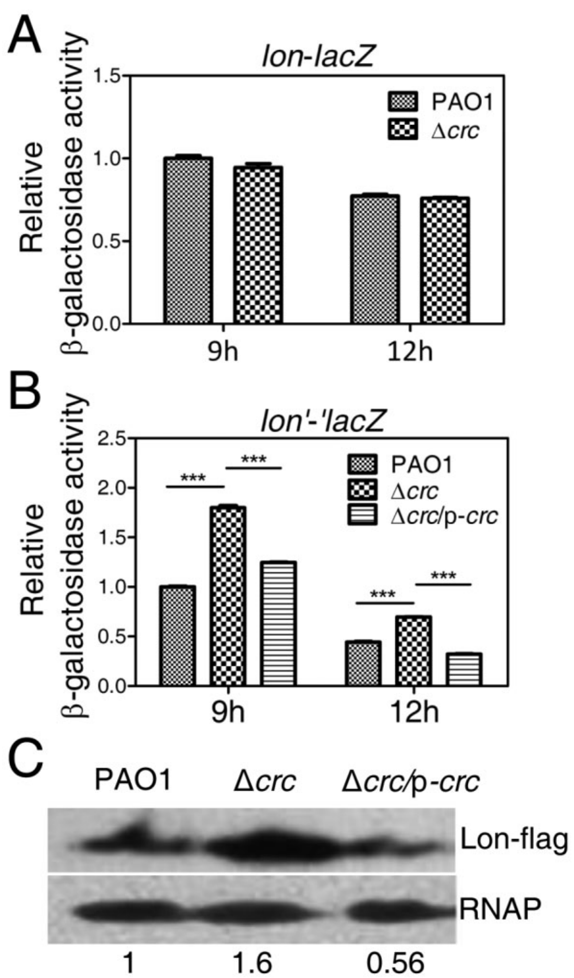

Fig. 5. Effect of *crc* deletion on the expression of *lon*.
A. Transcriptional *lon-lacZ* fusion constructs (*lon-lacZ*) in wild-type PAO1 and Δ*crc* backgrounds reveal no significant increase of *lon-lacZ* activity in the Δ*crc* background.
B. The absence of *crc* gene results in a significant increase of *lon* translational activity. ***$P < 0.001$ (*t*-test).
C. The absence of the *crc* gene results in an increase in Lon-flag protein. Expression of Lon-flag was normalized to RNAP and the results are reported as fold changes with control bacteria PAO1 set to 1. In A, B and C, bacteria were grown in M8 minimal medium at 37°C with shaking (250 r.p.m.). In A and B, the results were normalized to OD_{600}. Values represent means ± standard error of the mean (SEM) and each value was performed with triplicate biological replicates.

Like Crc, Hfq represses lon *gene expression at the posttranscriptional level*

Recent observations suggest that the Crc protein is devoid of RNA-binding activity and that it has an ancillary role in Hfq-mediated regulation (Milojevic *et al*., 2013; Moreno *et al*., 2014; Sonnleitner and Blasi, 2014). We noted that the *lon* mRNA features an AU-rich sequence covering the translational start site (AUU<u>AUG</u>AAAA, the underlined AUG is the start codon of *lon*). We next asked whether Hfq is involved in the posttranscriptional regulation of Lon, given that Hfq protein preferentially binds AU-rich sequences in single-stranded regions and represses translation (Vogel and Luisi, 2011; Sonnleitner and Blasi, 2014). As shown in Fig. 6, the β-galactosidase activity conferred by the transcriptional *lon-lacZ* fusion was comparable in strains PAO1, Δ*hfq* and Δ*crc*Δ*hfq* (Fig. 6A), suggesting that Hfq has no significant effect on *lon* transcription. However, the deletion of *hfq* in wild-type PAO1 increases the synthesis of the Lon-LacZ fusion protein by approximately 150% (Fig. 6B). When complemented with a plasmid carrying a wild-type *hfq* gene (p-*hfq*, Supporting Information Table S1), the expression of translational *lon'-'lacZ* fusion was restored to wild-type levels in Δ*hfq* mutants (Fig. 6B). In addition, we also observed that deletion of *hfq* resulted in a 1.82-fold increase in the expression of Lon-flag (Fig. 6C). These results suggest that Hfq inhibits the expression of Lon at a posttranscriptional level.

Next, we tested whether Hfq directly binds to *lon* mRNA. A gel-shift assay was performed with purified Hfq and a *lon* mRNA fragment ($lon_{-215\ to\ +236}$) covering nucleotides form −215 to +236 with regard to the A (+1) of start codon. This experiment revealed that Hfq could bind to *lon* mRNA ($lon_{-215\ to\ +236}$), forming a stable protein-RNA complex (Fig. 6D). Using RNase I footprinting analysis, we observed that the purified 6His-Hfq was capable of protecting a region that covers nucleotide position −7 to +12 with regard to the A (+1) of the *lon* start codon from RNase I digestion (Supporting Information Fig. S5). This Hfq-protected region is adjacent to the putative ribosome-binding site of *lon* (Supporting Information Fig. S5), supporting the notion that Hfq may be involved in the regulation of *lon* mRNA translation (Fig. 6).

The Hfq-binding site on *lon* mRNA covers an AU-rich sequence AUU<u>AUG</u>AAAA (the underlined AUG is the start codon of *lon*) (Supporting Information Fig. S5). We next asked whether this AU-rich sequence is involved in the interaction between Hfq and the $lon_{-215\ to\ +236}$ mRNA. To this end, we mutated the second codon of *lon* (AUUAUG<u>AAA</u>A, the underlined AAA was mutated as GCC, yielding A456-GCC mutant) and performed Electrophoretic Mobility Shift Assay (EMSA) again. As shown in Supporting Information Fig. S6, A456-GCC mutation abolished the formation of stable protein-RNA complexes to a certain degree, suggesting that the AU-rich sequence contributes to the interaction between Hfq and the *lon* mRNA. Taken together, these results suggest that Hfq represses *lon* gene expression at the posttranscriptional level in a direct manner.

Crc contributes to Hfq-mediated regulation of lon

In line with previous studies suggesting that Crc protein is devoid of RNA-binding activity (Milojevic *et al*., 2013; Moreno *et al*., 2014; Sonnleitner and Blasi, 2014), we

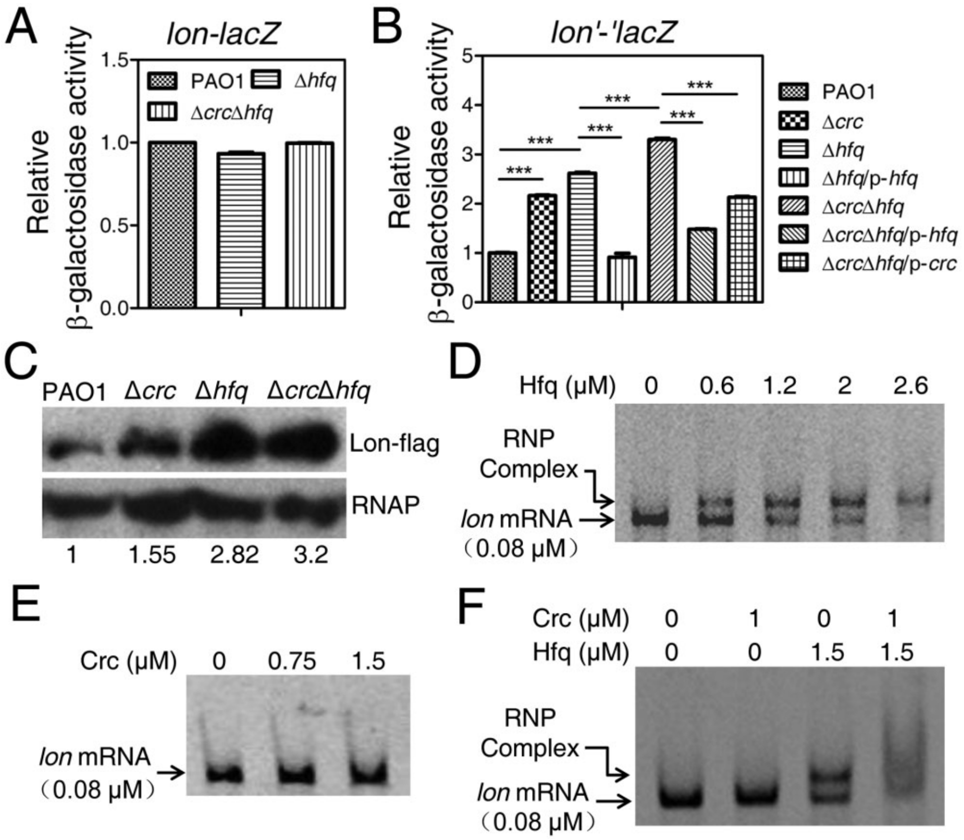

Fig. 6. Crc contributes to Hfq-mediated regulation. In all panels, PAO1, Δ*crc*, Δ*hfq* and Δ*crc*Δ*hfq* harbor plasmid PAK1900 respectively.
A. Expression of transcriptional *lon-lacZ* fusion in wild-type PAO1, Δ*hfq* and Δ*crc*Δ*hfq* backgrounds.
B. Expression of translational *lon'-'lacZ* fusion in wild-type PAO1 and its derivatives. In A and B, bacteria were grown in M8 minimal medium at 37°C for 9 h with shaking (250 r.p.m.); values represent means ± standard error of the mean (SEM) and each value was performed with triplicate biological replicates. $^{***}P < 0.001$ (*t*-test).
C. The expression of Lon-flag was measured in PAO1 and its derivatives when bacteria were grown in M8 minimal medium at 37°C for 9 h with shaking (250 r.p.m.). The results were normalized to RNAP and reported as fold changes with control bacteria PAO1 set to 1.
D, E and F. Ribonucleoprotein (RNP) complexes formed in the presence of the lon mRNA ($lon_{-215\ to\ +236}$) and either 6His-Hfq (D), 6His-Crc (E), or both 6His-Hfq and 6His-Crc (F). 6His-Crc and 6His-Hfq were added at the indicated concentrations (expressed as monomers). RNA and protein-RNA complexes were resolved in a non-denaturing polyacrylamide gel. The position of free RNA and of the RNP complexes detected is indicated.

observed that purified 6His-Crc protein (> 95% pure, Supporting Information Fig. S7) is unable to bind *lon* mRNA ($lon_{-215\ to\ +236}$) at a low micromolar range (1.5 μM) (Fig. 6E). When Hfq (1.5 μM) is presented alone, we observed certain degrees (approximately 50%) of shift in *lon* mRNA ($lon_{-215\ to\ +236}$) (Fig. 6F). When both Hfq (1.5 μM) and Crc (1 μM) were present, nearly all *lon* mRNA ($lon_{-215\ to\ +236}$) (0.08 μM) exhibited a slow electrophoretic mobility, generating a smear (Fig. 6F). The *Escherichia coli* Hfq contamination in the 6His-Crc protein sample is about 0.1% (approximately 0.001 μM in EMSA, expressed as monomers) (Supporting Information Fig. S7B), and therefore it is unlikely to be responsible for the slow electrophoretic mobility of the *lon* mRNA (0.08 μM) when together with 1.5 μM of purified Hfq (Fig. 6F), given that approximately half of *lon* mRNAs (0.04 μM) remain unshifted in our gel-shift assay in the presence of 1.5 μM of purified Hfq alone (Fig. 6F). Thus, these observations indicate a potential co-action of Hfq and Crc in generating the high affinity stable complex with *lon* mRNA, which is in line with recent studies showing that Crc and Hfq form co-riboprotein complexes with either *dmpR* mRNA (Madhushani *et al.*, 2014) or *alkS* mRNA (Moreno *et al.*, 2014).

As shown in Fig. 6, deletion of *crc* in the wild-type PAO1 background increased the expression of both *lon'-'lacZ* fusion and Lon-flag while the expression was at a lower level than measured for the *hfq* deletion mutant (Δ*hfq*) (Fig. 6B and C). Moreover, in contrast to the major difference observed between the wild-type and Δ*hfq* mutant, lack of Crc in the Δ*hfq* background only had a minor effect on the expression of either *lon'-'lacZ* fusion (Fig. 6B) or Lon-flag (Fig. 6C). These observations indicate that Hfq

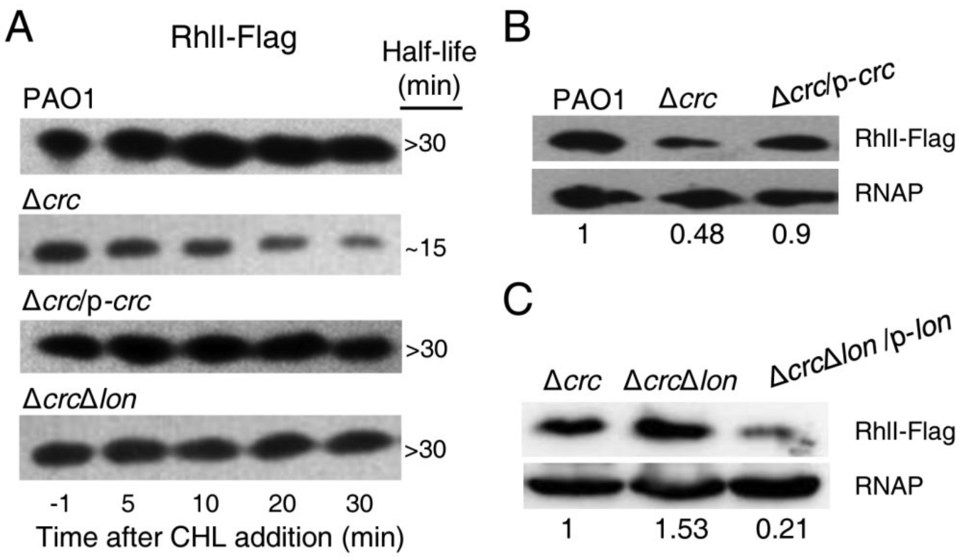

Fig. 7. Crc modulates the stability and abundance of RhlI protein in a manner opposite to Lon. In all panels, PAO1, Δ*crc* and Δ*crc*Δ*lon* harbor plasmid PAK1900 respectively.
A. The stability of RhlI-flag protein from PAO1, Δ*crc*, Δ*crc*/p-*crc* and Δ*crc*Δ*lon* strains was analyzed using *in vivo* degradation experiments and Western blot analysis. Chloramphenicol (CHL) was used to block translation and sampled at time points thereafter.
B. The abundance of RhlI-flag in PAO1 and its derivatives was analyzed using Western blot analysis. Results are reported as fold changes with control bacteria PAO1 set to 1.
C. The abundance of RhlI-flag in Δ*crc*, Δ*crc*Δ*lon* and Δ*crc*Δ*lon*/p-*lon* strains was analyzed using Western blot analysis. Results are reported as fold changes with control bacteria Δ*crc* set to 1. All experiments were repeated at least three times with similar results and the figures show a set of representative data.

exerts a more pronounced negative effect on the posttranscriptional regulation of *lon* than Crc, which is also in line with the notion that Hfq is required to enable Crc to mediate a repressive effect on translation (Sonnleitner and Blasi, 2014). Thus, it is likely that Crc contributes to Hfq-mediated regulation of Lon expression at a posttranscriptional level.

Lon is primarily required for the Crc-modulated proteolysis of RhlI in vivo

As aforementioned, deletion of *crc* resulted in the up-regulation of *lon* at a posttranscriptional level (Figs 5 and 6). Because Lon is a protease involved in proteolytic processes (Gottesman, 1996; Gottesman *et al*., 1997; Wickner *et al*., 1999) and is unlikely to degrade the RhlR protein (Takaya *et al*., 2008), we next examined whether Crc affects the degradation of RhlI by determining the *in vivo* half-life of the RhlI-flag protein in a wild-type PAO1 strain, a *crc* deletion strain (Δ*crc*), a complementary strain (Δ*crc*/p-*crc*) and a *crc lon* double mutant strain (Δ*crc*Δ*lon*) as described in previous studies (Langklotz *et al*., 2011; Maisonneuve *et al*., 2013). Bacterial cultures were treated with the antibiotic chloramphenicol in order to block translation, and sampled at time points thereafter. Western blot analysis for RhlI-flag using an anti-FLAG antibody showed an RhlI-flag degradation over time. Our data revealed that over the 30 min period tested, the abundance of the RhlI-flag protein remained high in both the wild-type PAO1 strain and the complementary strain (Δ*crc*/p-*crc*) with a half-life greater than 30 min (Fig. 7A). However, the half-life of RhlI-flag was approximately 15 min in the *crc* deletion strain (Δ*crc*) (Fig. 7A). These data demonstrate that RhlI is less stable in the absence of *crc*. Moreover, the half-life of RhlI-flag protein in the *crc lon* double mutant strain (Δ*crc*Δ*lon*) was longer than 30 min (Fig. 7A), suggesting that the additional disruption of *lon* suppresses the decrease of RhlI protein stability caused by *crc* disruption. Thus, it is likely that Crc positively controls the protein stability of RhlI by repressing Lon.

To examine whether Crc affects the abundance of RhlI *in vivo*, we next performed Western blot analysis. As shown in Fig. 7B, the level of RhlI-flag was decreased approximately by 52% in the *crc* deletion strain (Δ*crc*) as compared with that of wild-type PAO1. Providing a wild-type copy of *crc* works to suppress the decrease in the abundance of RhlI-flag by *crc* deletion (Fig. 7B), suggesting that Crc positively modulates the cellular level of RhlI. Next, we analyzed the effect of *lon* disruption on the cellular level of RhlI-flag in a *crc*-disrupted background. As shown in Fig. 7C, the *lon* disruption increased RhlI-flag abundance by approximately 53%. When the *crc lon* double mutant strain (Δ*crc*Δ*lon*) was transformed by a high copy number of the cloned *lon* gene (p-*lon*, Support-

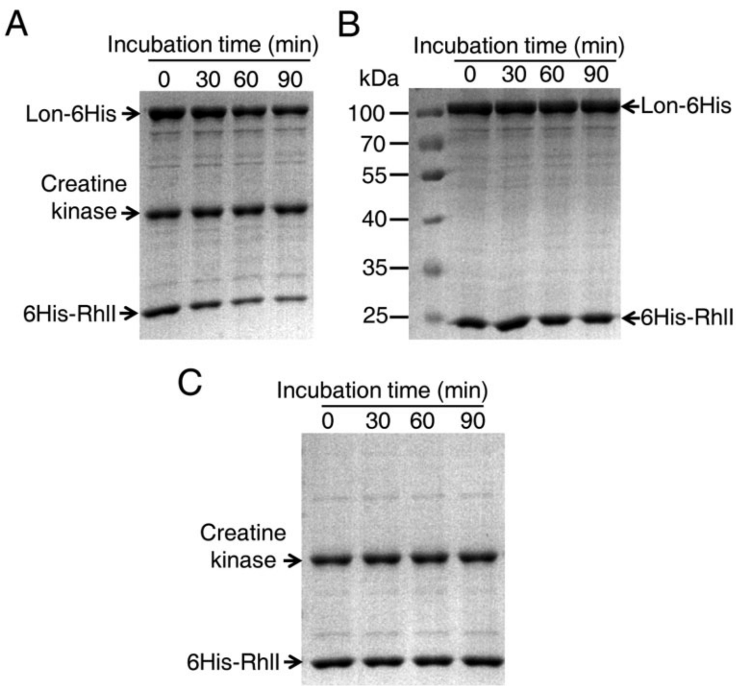

Fig. 8. *In vitro* degradation of RhlI by Lon.
A. *In vitro* proteolysis assay showing that Lon-6His degrades 6His-RhlI. Creatine kinase, present in the reaction mixture, was used as a loading control.
B. *In vitro* proteolysis assay showing that Lon-6His fails to degrade 6His-RhlI in the absence of ATP and an ATP regeneration system.
C. *In vitro* proteolysis assay showing that 6His-RhlI is stable in the presence of ATP and an ATP regeneration system without Lon-6His. Protein samples taken at indicated time points were resolved on 10% polyacrylamide Tris-tricine gel followed by Coomassie blue staining. All experiments were repeated at least three times with similar results and the figures show a set of representative data.

ing Information Table S1), the RhlI-flag was present at very low levels relative to either the Δ*crc* or the Δ*crc*Δ*lon* strains (Fig. 7C), suggesting that *lon* is a negative regulator of the abundance of RhlI protein. Therefore, it is possible that Crc modulates the abundance of RhlI via the Lon protease, which also suggests that the Lon-mediated proteolysis of RhlI (Fig. 7A) may contribute to the abundance of RhlI.

Moreover, we observed that deletion of *hfq*, which resulted in up-regulation of *lon* at posttranscriptional level (Fig. 6), also significantly reduced the *in vivo* stability (Supporting Information Fig. S8A) and abundance of RhlI protein (Supporting Information Fig. S8B), as well as the C4-HSL content (Supporting Information Fig. S8C). These results further substantiated our conclusion that Lon-mediated proteolysis of RhlI is important for the regulation of *rhl* QS. Additionally, it has been reported that Hfq contributes to *rhlI* expression through stabilization of the non-coding RNA RsmY (Sonnleitner *et al*., 2006; Sorger-Domenigg *et al*., 2007). Thus, Hfq may modulate *rhl* QS via multiple pathways.

Lon degrades RhlI protein in vitro

Although the role of the Lon protease in *P. aeruginosa* has not yet been studied in depth, it appears to be a master regulator of the complex adaptations of this pathogen (Brazas *et al*., 2007; Marr *et al*., 2007; Takaya *et al*., 2008; Breidenstein *et al*., 2012). So far, the LasI protein is the only known *in vivo* substrate for Lon of *P. aeruginosa* (Takaya *et al*., 2008). As aforementioned, Lon was the protease primarily responsible for the *in vivo* degradation of RhlI in the Δ*crc* mutant (Fig. 7A). Therefore, we next sought to test whether Lon is capable of digesting RhlI in an *in vitro* system, containing purified 6His-RhlI, Lon-6His, ATP and a system for ATP regeneration. As shown in Fig. 8A, 6His-RhlI was degraded with a half-life of approximately 30 min *in vitro*, confirming our findings obtained *in vivo* (Fig. 7A). In line with the notion that efficient degradation of protein substrates by Lon requires the binding and hydrolysis of ATP (Gottesman, 1996; Gottesman *et al*., 1997; Wickner *et al*., 1999), we observed that the degradation of 6His-RhlI was indeed dependent on the presence of ATP and the ATP regeneration system (Fig. 8B). As expected, 6His-RhlI is stable in the presence of ATP and an ATP regeneration system without Lon-6His (Fig. 8C). These results suggest that the degradation of 6His-RhlI is specific to the addition of Lon to the reaction buffer. To our knowledge, this is the first demonstration of an *in vitro* substrate for the Lon protease of *P. aeruginosa*.

Constitutive expression of rhlI suppresses the defects of a crc deletion mutant

As deletion of *crc* resulted in decreased production of rhamnolipid and *rhl* QS signal C4-HSL (Figs 1 and 2), we asked whether the constitutive expression of *rhlI* (encoding RhlI protein that synthesizes the C4-HSL) in the *crc* deletion mutant strain (Δ*crc*) suppresses the defect of the Δ*crc* strain in the production of either rhamnolipid or C4-HSL. We constructed a plasmid for the constitutive expression of *rhlI* (p-*rhlI*, Supporting Information Table S1)

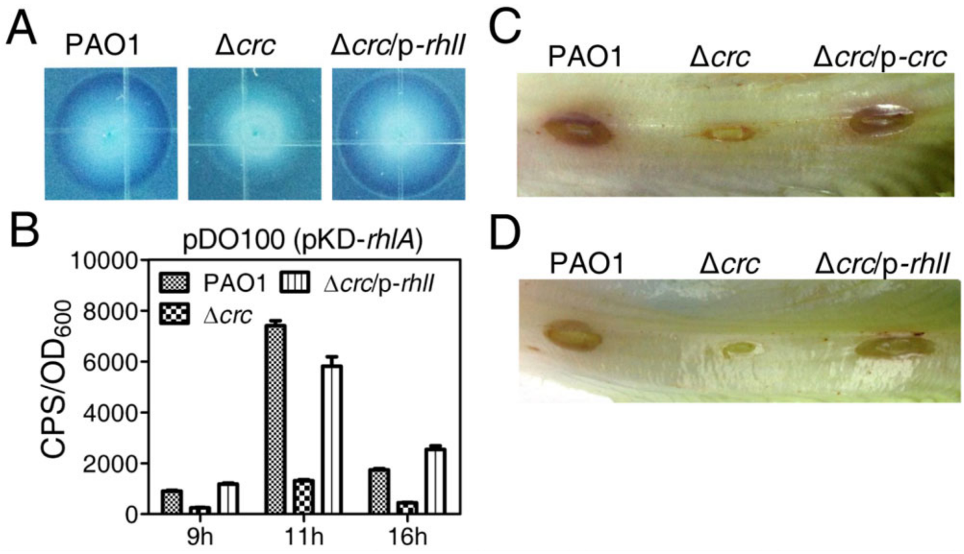

Fig. 9. Constitutive expression of *rhlI* suppresses the defects of *crc* deletion mutant. In all panels, PAO1 and Δ*crc* harbor plasmid PAK1900 respectively.
A. PAO1 and its derivates were inoculated onto a CTAB plate and incubated at 37°C for 24 h and then for 48 h at room temperature.
B. Relative amount of C4-HSL measured by the pDO100 (pKD-*rhlA*) system. Bacteria were grown in M8 minimal medium at 37°C for 9 h with shaking (250 r.p.m.) and supernatants were subsequently prepared. The results were normalized to OD_{600} and values represent means ± standard error of the mean (SEM), and each value was performed with triplicate biological replicates.
C and D. Photographs show lettuce midribs after 3 days of infection with *Pseudomonas aeruginosa* PAO1 and its derivates. Results are representative of three independent experiments.

and then introduced it into the *crc* deletion mutant (Δ*crc*), yielding the Δ*crc*/p-*rhlI* strain. As shown in Fig. 9A and B, the Δ*crc*/p-*rhlI* strain displayed wild-type levels of rhamnolipid and C4-HSL production, suggesting that the decreased abundance of RhlI (Fig. 7B) may be responsible for the reduced levels of both rhamnolipid and C4-HSL in the Δ*crc* strain.

Deletion of *crc* led to the attenuation of *rhl* QS (Figs 1 and 2), indicating that Crc might have significant implications for the ability of *P. aeruginosa* to cause disease as the *rhl* QS system is an important regulator of the pathogenesis of this pathogen (Rumbaugh *et al.*, 1999; Smith and Iglewski, 2003; Zhu *et al.*, 2004; Kohler *et al.*, 2010; Rutherford and Bassler, 2012; O'Loughlin *et al.*, 2013; Cao *et al.*, 2014). We next tested the effect of the *crc* deletion on virulence of *P. aeruginosa* using a lettuce infection model (Rahme *et al.*, 1997; Goldova *et al.*, 2011; Cao *et al.*, 2014). Relative to wild-type PAO1, the Δ*crc* strain failed to cause severe necrotic lesions of the leaves, which can be complemented by introducing a wild-type *crc* gene into the Δ*crc* strain (Fig. 9C). This reveals that the *crc* mutant is less virulent than the wild types. Again, we found that the constitutive expression of *rhlI* in the Δ*crc* strain could restore the virulence to wild-type levels (Fig. 9D), suggesting that the decreased abundance of RhlI (Fig. 7B) is likely responsible for the attenuated virulence of the Δ*crc* strain in this lettuce leaf model of *P. aeruginosa* infection.

Discussion

The Crc protein is a mediator of the CCR system that enables *Pseudomonas* to adapt quickly to a preferred carbon and energy source (Gorke and Stulke, 2008; Rojo, 2010; Rabinowitz and Silhavy, 2013; Moreno *et al.*, 2014; Sonnleitner and Blasi, 2014). In this study, we showed that the Crc protein participates in the down-regulation of the Lon gene to promote *rhl* QS in *P. aeruginosa*. A proposed model for the role of Crc in the regulation of *rhl* QS is shown in Fig. 10.

In *Pseudomonas* species, Crc contributes to Hfq-mediated regulation (Sonnleitner and Blasi, 2014). In line with this study, we found that Crc contributes to Hfq-mediated repression of *lon* gene expression at posttranscriptional level (Fig. 6). Crc has slight effects on the expression of both *lon'*-*'lacZ* fusion and Lon-flag in strains lacking Hfq (Fig. 6 and Supporting Information Fig. S9), and this observation is consistent with a recent study showing that lack of Crc in an Hfq-null background had a minor effect on the translation of *dmpR* in *Pseudomonas putida* (Madhushani *et al.*, 2014). However, these effects are minor and thus making them and their physiological relevance somewhat questionable. In addition, it seems that Crc increases the affinity or the stability in a Crc/Hfq/RNA complex for some specific RNAs (Madhushani *et al.*, 2014; Moreno *et al.*, 2014) (Fig. 6) and hence provides the

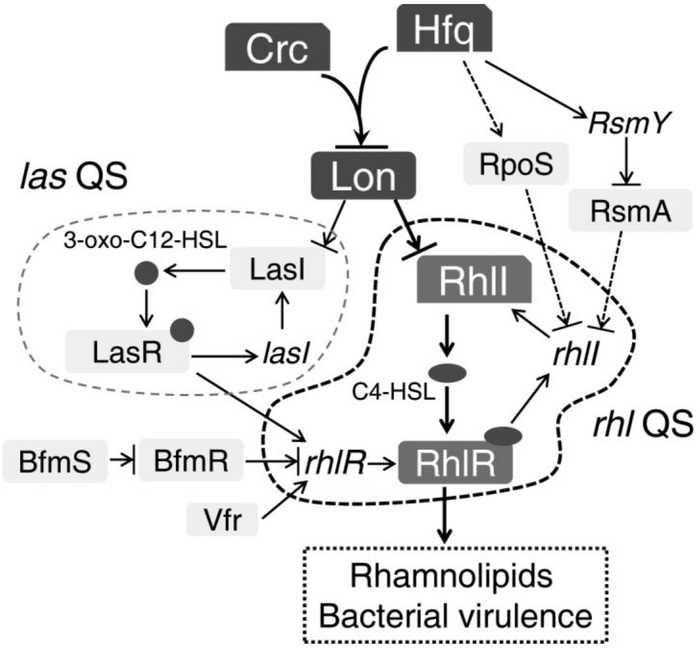

Fig. 10. A model of Crc-Hfq/Lon/RhlI gene regulatory cascade involved in the regulation of *rhl* QS in *Pseudomonas aeruginosa*. The lines show the interaction between the players: arrow, activation; hammerheads, repression; solid line, a direct influence or direct connection; and dotted line, a putative or indirect connection. The *las* QS and *rhl* QS systems are indicated by dotted and closed lines respectively. This model is based on the results of the current study and some previous studies (Whiteley *et al*., 2000; Sonnleitner *et al*., 2003; 2006; Schuster and Greenberg, 2006; Sorger-Domenigg *et al*., 2007; Croda-Garcia *et al*., 2011; Rutherford and Bassler, 2012; Cao *et al*., 2014). Details are seen in the main text.

biological specificity required for a proficient regulation of *Pseudomonas* metabolism in the presence of different carbon sources (Madhushani *et al*., 2014; Moreno *et al*., 2014). Thus, the details of Crc-mediated gene regulation await further investigation. It is presently unknown what the mode of action of Crc in gene expression regulation is and whether there is a single mechanism used by all. Nonetheless, our results suggest that Hfq exerts a more pronounced negative effect on *lon* gene expression than Crc and that Crc plays an ancillary role (Fig. 6 and Supporting Information Fig. S9).

We showed that Lon modulates the *in vivo* and *in vitro* degradation of RhlI protein that synthesizes the *rhl* QS signal C4-HSL and may thus affect *rhl* QS and rhamnolipid production (Fig. 10). A previous study illustrating that *rhl* QS is down-regulated by Lon in a *las*-dependent and *las*-independent manner supports this hypothesis (Takaya *et al*., 2008). In addition, constitutive expression of *rhlR*, but not *lasR* (encoding the master regulator of *las* QS system), can completely suppress the rhamnolipid defect caused by the deletion of *crc* (Supporting Information Fig. S10), suggesting that the *P. aeruginosa rhl* QS system likely has a more profound effect on rhamnolipid production than the *las* QS system under our experimental conditions. Moreover, it has been reported that under some conditions (Dandekar and Greenberg, 2013), for example, those employed for the rhamnolipid assay, the *rhl* QS system is independent of the *las* QS system (Gupta *et al*., 2009).

We found a small decrease (less than 45%) in either *rhlR* or *rhlI* transcription in the *crc* deletion mutant compared with wild-type PAO1 strain (Supporting Information Table S5). It remains to be determined if this small difference has an important effect on the significant physiological consequences (Figs 1, 2 and 9). Given that the *rhl* QS system is a subordinate to the *las* QS system and that the regulation of the *rhl* QS system is complex (Schuster and Greenberg, 2006; Rutherford and Bassler, 2012), Lon-mediated protein degradation of LasI (Takaya *et al*., 2008) and not-yet-identified factors may contribute to the decrease of either *rhlR* or *rhlI* transcription in the Δ*crc* strain (Fig. 10). Alternatively, the decreased expression of *rhlR* and *rhlI* may be a result of reduced C4-HSL content as caused by the low stability of the RhlI protein, which in turn affects the transcription of *rhlR* and *rhlI* (Fig. 10). These hypotheses, however, will require further investigation.

Besides affecting the abundance and stability of RhlI via Lon, Crc may modulate *rhl* QS and rhamnolipid production via the *pqs* QS system (Zhang *et al*., 2013) as well as in other as-yet-unidentified ways. We found that ClpX, which acts as a negative regulator of the *rhl* QS system (Fig. 4), is also required for Crc to exert its role on *rhl* QS (Fig. 3B and D). ClpX is an alternative ATP-binding subunit of the Clp protease (Gottesman, 1996; Gottesman *et al*., 1997; Wickner *et al*., 1999), although its detailed biological functions remain to be elucidated in *P. aeruginosa* (Qiu *et al*., 2008). In *E. coli*, the PQC proteases Lon and ClpXP are responsible for 60% of the total protein degradation in growing cells (Maurizi, 1992). Further studies are needed to explore the functional relationship between *crc*, *clpX* and *rhl* QS. Nonetheless, these results suggest that the PQC system plays pivotal roles in linking the CCR system with *rhl* QS in *P. aeruginosa*.

Pseudomonas aeruginosa PAO1 lacking Crc exhibited attenuated virulence in lettuce leaf (Fig. 9C and D). This result is consistent with a previous study that reported a PAO1 Δ*crc* strain is less virulent in a *Dictyostelium discoideum* model (Linares *et al.*, 2010). Additionally, we observed that inactivation of Crc decreases *P. aeruginosa* proliferation in mouse lungs (Supporting Information Fig. S11), confirming an important role of Crc in *P. aeruginosa* pathogenesis. However, this result is inconsistent with a recent study in which the *P. aeruginosa* PA14 Δ*crc* strain exhibited a higher bacterial load than the wild-type PA14 in lungs in a mouse lung infection model (Zhang *et al.*, 2013). This discrepancy may be due to the utilization of different mouse infection models or as a consequence of the different genetic backgrounds of the PAO1 and PA14 strains. Although the reason for this discrepancy remains unknown, it is clear that Crc has a significant impact on the pathogenesis of *P. aeruginosa* (Fig. 9 and Supporting Information Fig. S11) (Linares *et al.*, 2010; Zhang *et al.*, 2013).

In summary, here we identified a previously unexplored posttranscriptional regulatory cascade, Crc-Hfq/Lon/RhlI, for the regulation of rhamnolipid production, *rhl* QS and bacterial virulence in *P. aeruginosa* (Fig. 10). We also demonstrated that the PQC systems are crucial for the regulation of *rhl* QS in *P. aeruginosa*. Dissecting virulence pathways of *P. aeruginosa* may ultimately lead to a better understanding of the bacterium's pathogenicity, which will contribute to the development of novel strategies to combat the dreaded *P. aeruginosa* infectious disease.

Experimental procedures

Bacterial strains, plasmids and culture conditions

Supporting Information Table S1 lists the bacterial strains and plasmids used in this study. Unless otherwise noted, *P. aeruginosa* PAO1 and its derivatives were grown in Luria-Bertani (LB) broth or M8 salt-based medium supplemented with 0.3% succinate (m/v), 2 mM $MgSO_4$ and 0.05% glutamate (termed here M8 minimal medium, for convenience) (Kohler *et al.*, 2000). *E. coli* cultures were grown in LB broth; cultures were incubated at 37°C with shaking (250 r.p.m.). For plasmid maintenance, antibiotics were used at the following concentrations where appropriate: for *E. coli*, carbenicillin at 100 μg ml^{-1}, kanamycin at 50 μg ml^{-1}, tetracycline at 5 μg ml^{-1} and gentamicin at 10 μg ml^{-1}; for *P. aeruginosa*, gentamicin at 30 μg ml^{-1} in LB or 100 μg ml^{-1} in *Pseudomonas* Isolation Agar (PIA; BD); tetracycline at 30 μg ml^{-1} in LB and/or 100 μg ml^{-1} in PIA; carbenicillin at 100 μg ml^{-1} in LB, M8 minimal medium and PIA; trimethoprim at 300 μg ml^{-1} in LB, M8 minimal medium and PIA; and kanamycin at 200 μg ml^{-1} in LB, M8 minimal medium and PIA.

Transposon mutagenesis

The PAO1::*rhlA-lacZ* and Δ*crc*::*Tc* were subjected to transposon mutagenesis using the mariner transposon vector pBT20 (Kulasekara *et al.*, 2005). The transposon in pBT20 was conjugally transferred by biparental mating into *P. aeruginosa*, following a protocol previously described (Kulasekara *et al.*, 2005). Briefly, the donor strain (*E. coli* SM10-λ *pir*) containing the pBT20 and the recipient PAO1 or Δ*crc*::*Tc* strain were scraped from overnight plates and resuspended in 1 ml of M8 minimal medium. Concentrations of the bacteria in the suspensions were adjusted to OD_{600} of 40 for the donor and OD_{600} of 20 for the recipient. Next, each donor and recipient was mixed together and spotted on a dry LB agar plate and incubated at 37°C for 7 h. Mating mixtures were scraped and resuspended in 1 ml of M8 minimal medium. Transposon-mutagenized bacteria were selected by plating on PIA plates containing gentamicin at 100 μg ml^{-1}. Each round of mutagenesis yielded about 50 000 colonies. A sterile toothpick was used to pick up individual colonies and dip them into the CTAB agar plates. Colonies were visually scored for the size of the blue halo surrounding the colonies when bacteria were grown on the CTAB agar plates; the blue halo indicates the production of rhamnolipids (Kohler *et al.*, 2000; Gupta *et al.*, 2009). Approximately 50 000 to 55 000 colonies were inoculated onto CTAB plates and were screened for the appearance of rhamnolipid production for PAO1::*rhlA-lacZ* insertion mutants and Δ*crc*::*Tc* insertion mutants respectively. The localization of the Mariner transposon with respect to the *P. aeruginosa* genome was determined using an established protocol (Kulasekara *et al.*, 2005).

Construction of vectors

Plasmids p-*crc*, p-*lon*, p-*lon-F*, p-*clpX*, p-*rhlI*, p-*rhlR*, p-*hfq*, p-*lasR* and p-*PA2458* were constructed respectively by amplifying corresponding fragments with primer pairs (Supporting Information Table S2) *crc*-comp-F/*crc*-comp-R (*Hin*dIII/*Bam*HI), *lon*-comp-F/*lon*-comp-R (*Xba*I/*Hin*dIII), lon-OE-F/lon-OE-R (*Hin*dIII/*Xba*I), *clpx*-comp-F/*clpx*-comp-R (*Hin*dIII/*Bam*HI), rhlI-OE-F/rhlI-OE--R (*Hin*dIII/*Bam*HI), rhlR-OE-F/rhlR-OE-R (*Hin*dIII/*Hin*dIII), *hfq*-comp-F/*hfq*-comp--R (*Hin*dIII/*Bam*HI), *lasR*-OE-F/*lasR*-OE-R (*Hin*dIII/*Bam*HI) and *PA2458*-comp-F/*PA2458*-comp-R (*Hin*dIII/*Bam*HI) by PCR. The PCR products were digested with the indicated enzymes and cloned into PAK1900 (Jansons *et al.*, 1994). In p-*crc*, p-*lon-F*, p-*clpX*, p-*rhlI*, p-*rhlR*, p-*hfq*, p-*lasR* and p-*PA2458*, the direction of transcription of the cloned genes is in the same orientation as p*lac*. In p-*lon*, the transcription of *lon* gene occurs in the opposite direction of the orientation of p*lac*.

lacZ promoter fusions were made at the CTX phage attachment site in *P. aeruginosa* by using the vector systems of mini-CTX-lacZ (Becher and Schweizer, 2000) and mini-CTX-lacZ-EB (Irie *et al.*, 2010). The plasmid mini-CTX-lacZ was used to construct transcriptional LacZ fusion while the mini-CTX-lacZ-EB was used to construct translational LacZ fusion. For generating transcriptional fusion *lon-lacZ*, the *lon* promoter region (−333 to −20 of the start codon) was amplified by PCR using primer pair *lon-lacZ*-F/*lon-lacZ*-R1 (Supporting Information Table S2) and cloned into the mini-ctx-lacZ plasmid. For generating translational fusion *lon'-'lacZ*, a 413 bp PCR product (−333 to +80 of the *lon* start codon) was amplified by PCR using primer pair (Supporting Information Table S2) *lon-lacZ*-F/*lon'-'lacZ*-R2 and cloned into mini-CTX-lacZ-EB. For generating transcriptional fusion *rhlA-lacZ*, *rhlA* promoter region (–591 to –10 of the start codon) was amplified by PCR using primer pair (Supporting Information Table S2) *rhlA-lacZ*-F/*rhlA-lacZ*-R and subsequently cloned into the mini-ctx-lacZ plasmid.

Primer pairs lon-flag-F/lon-flag-R (*Eco*RI/*Hin*dIII) and rhlI-flag-F/rhlI-flag-R (*Sal*I/*Hin*dIII) were used to amplify the *lon* and *rhlI* genes that were intended to fuse with a C-terminal Flag-tag respectively. The indicated enzymes that digested the PCR products were cloned into the corresponding enzyme sites of mini-CTX-lacZ to generate either mini-ctx-*lon-flag* or mini-ctx-*rhlI-flag*.

All constructs were sequenced to ensure that no unwanted mutations resulted.

Construction of P. aeruginosa Δcrc*,* Δcrc::Tc*,* Δlon*,* ΔclpX*,* ΔcrcΔlon*,* Δhfq *and* ΔcrcΔhfq *mutants*

For gene replacement, a SacB-based strategy (Hoang *et al*., 1998) was employed as described in previous studies (Lan *et al*., 2010; Cao *et al*., 2014). To construct the *crc*-null mutant (Δ*crc*), PCRs were performed to amplify sequences upstream (966 bp) and downstream (885 bp) of the intended deletion. The upstream fragment was amplified from PAO1 genomic DNA using primer pair D-crc-up-F/D-crc-up-R (*Eco*RI/*Bam*HI) (Supporting Information Table S2), while the downstream fragment was amplified with primer pair D-crc-down-F/D-crc-down-R (*Bam*HI/*Hin*dIII) (Supporting Information Table S2). The two PCR products were digested and then cloned into *Eco*RI/*Hin*dIII-digested gene replacement vector pEX18Ap, yielding pEX18Ap::*crc*UD. A ca. 1.8 kb gentamicin resistance cassette cut from pPS858 with *Bam*HI was cloned into pEX18Ap::*crc*UD, yielding pEX18Ap::*crc*UGD. The resultant plasmids were electroporated into PAO1 with selection for gentamicin resistance. Colonies showing both gentamicin resistance and loss of sucrose (10%) susceptibility were selected on LB agar plates containing 30 μg ml^{-1} of gentamicin and 10% sucrose, which typically indicates a double cross-over event and thus of gene replacement occurring. The Δ*crc*::*Tc* mutant was constructed by a similar strategy as described above. A ca. 2.3 kb tetracycline resistance cassette was amplified from the integration vector mini-CTX-lacZ with primer pair Mini-TC-F/Mini-TC-R (with *Bam*HI site) (Supporting Information Table S2) for replacing the *crc* gene in PAO1. The Δ*crc* mutant was further confirmed by PCR.

For deletion of the *lon* gene in PAO1, the upstream fragment (ca. 1.8 kp) of the intended deletion was amplified with primer pair D-lon-up-F/D-lon-up-R (*Hin*dIII/*Bam*HI) (Supporting Information Table S2) while the downstream fragment (ca. 1.8 kp) was amplified with primer pair D-lon-down-F/D-lon-down-R (*Bam*HI/*Eco*RI). The ca. 2.3 kb tetracycline resistance cassette was cloned into pEX18Ap::lonUD, yielding pEX18Ap::lonUTD. For generating *crc lon* double deletion strain (Δ*crc*Δ*lon*), the *lon* gene in Δ*crc* mutant was deleted using a similar strategy with plasmid pEX18Ap::lonUTD. For deletion of *clpX* gene in PAO1, the upstream fragment (ca. 1.3 kp) of the intended deletion was amplified with primer pair D-clpx-up-F/D-clpx-up-R (*Eco*RI/*Bam*HI) while the downstream fragment (ca. 1kp) was amplified with primer pair D-clpx-down-F/D-clpx-down-R (*Bam*HI/*Hin*dIII) (Supporting Information Table S2). The ca. 1.8 kb gentamicin resistance cassette cut from pPS858 with *Bam*HI was cloned into pEX18Ap::clpxUD, yielding pEX18Ap::clpxUGD.

For deletion of the *hfq* gene in PAO1, the upstream fragment (ca. 0.96 kb) of the intended deletion was amplified with primer pair D-hfq-up-F/D-hfq-up-R (*Hin*dIII/*Bam*HI) (Supporting Information Table S2) while the downstream fragment (ca. 0.88 kb) was amplified with primer pair D-lon-down-F/D-lon-down-R (*Bam*HI/*Eco*RI). The two PCR products were digested and then cloned into the *Eco*RI/*Hin*dIII-digested gene replacement vector pEX18Ap, yielding pEX18Ap::*hfq*UD. A ca. 1.8 kb gentamicin resistance cassette cut from pPS858 with *Bam*HI was cloned into pEX18Ap::*hfq*UD, yielding pEX18Ap::*hfq*UGD. To construct the *crc hfq* double deletion strain (Δ*crc*Δ*hfq*) mutant, the plasmid pEX18Ap::*hfq*UGD was electroporated into Δ*crc* mutant from which the gentamicin resistance cassette was excised by using the plasmid pFLP2 that encoded Flp recombinase. The Δ*crc*Δ*hfq* mutant was selected as described above.

Construction of chromosomal-borne lon-flag*,* rhlI-flag*,* rhlA-lacZ*,* lon-lacZ *and* lon'-'lacZ *strains*

The resulting plasmids as described above were conjugated into *P. aeruginosa* PAO1 or its derivatives and the constructs integrated into the *attB* site as described previously (Becher and Schweizer, 2000; Irie *et al*., 2010) by a biparental mating using *E. coli* S17 λ-pir as donor. In these resulting strains except for PAO1::*rhlA-lacZ*, the mini-CTX plasmid backbone was excised by using the plasmid pFLP2 that encodes Flp recombinase. The Δ*crc*Δ*lon*::*rhlI-flag* strain was created in a PAO1::*rhlI-flag* background using plasmids pEX18Ap::*crc*UGD and pEX18Ap::lonUTD. The Δ*crc*Δ*lon*::*rhlI-flag* mutant was further confirmed by PCR.

β-galactosidase assays

Briefly, overnight cultures of the indicated strains were washed twice and diluted 80-fold in fresh M8 minimal medium. The liquid cultures were grown in a 20 ml tube with a tube volume-to-medium volume ratio of 5:1, shaking with 250 r.p.m. at 37°C, and sampled at time points thereafter. The β-galactosidase activity was assayed as previously described (Deng *et al*., 2012; Cao *et al*., 2014) using 4-methylumbelliferyl-β-d-galactoside (4MUG) as the enzymatic substrate. The product [7-hydroxy-4-methylcoumarin (4MU)] was detected using a 2104 EnVision® Multilabel Plate Readers or Synergy 2 (Biotek) following the manufacturer's instructions. The reaction was monitored at 460 nm with an excitation wavelength of 365 nm. Each sample was tested in triplicate. Relative LacZ activity was normalized by cell density at 600 nm.

Monitoring gene expression by lux*-based reporters*

The plasmid *rhlA-lux* (Supporting Information Table S1) was transformed into PAO1 and its derivatives by electroporation (Choi *et al*., 2006). Overnight cultures in LB medium of the indicated strains were washed and diluted 80-fold in M8 minimal medium in a 20 ml tube with a flask volume-to-medium volume ratio of 5:1. The liquid culture was grown at 37°C with shaking (250 r.p.m.). Promoter activities at different time points of bacterial growth were measured as counts per second (CPS) of light production with a Synergy 2 Multi-Mode Microplate Reader as described previously (Liang *et al.*, 2011; 2012; Cao *et al.*, 2014). Each sample was tested in triplicate. Relative light units were calculated by normalizing CPS to OD_{600}.

Detection and measurement of rhamnolipid production

Rhamnolipid production was estimated by inoculating strains on a CTAB agar plate as previously described (Kohler *et al.*, 2000, Gupta *et al.*, 2009, Cao *et al.*, 2014). The CTAB agar plate was based on M8 minimal medium supplemented with 0.0005% (m/v) methylene blue and 0.02% (m/v) CTAB, and was solidified with agar (1.6% final concentration). Individual colonies were picked up with a sterile toothpick and were dipped into a CTAB agar plate. The microorganisms were cultured at 37°C and the production of rhamnolipids resulted in the precipitation of CTAB, yielding a dark blue halo surrounding the colony.

To quantify the amount of rhamnolipids, the orcinol test was used as described previously (Liang *et al.*, 2011, Cao *et al.*, 2014). Overnight LB cultures of the indicated strains were washed and diluted 80-fold in 4 ml fresh M8 minimal medium in a 20 ml tube, 250 r.p.m. of aeration and at 37°C. After incubation for 48 h, 1 ml of the culture was centrifuged and the supernatant was extracted twice with 2 ml of diethyl ether. The pooled ether fractions were evaporated to dryness and the remainder was dissolved in 100 μl distilled water and mixed with 100 μl of 1.6% orcinol and 600 μl of 60% sulfuric acid. After heating for 30 min at 80°C in the dark, the samples were cooled for 15 min at room temperature and the absorbance at 421 nm (A421) was measured. The concentrations of rhamnolipids were calculated by comparing A421 values with those obtained for rhamnose standards between 0 and 1000 μg ml^{-1}, assuming that 1 μg of rhamnose corresponds to 2.5 μg of rhamnolipids.

Bioassay of C4-HSL activity

The assays were carried out on a black 96-well plate with a transparent bottom. An *rhlA* promoter-based *P. aeruginosa* strain pDO100 (pKD-*rhlA*) was used as previously described (Duan *et al.*, 2003; Liang *et al.*, 2011; 2012; Cao *et al.*, 2014). Briefly, the reporter strain pDO100 (pKD-*rhlA*) was grown overnight in LB medium at 37°C with shaking (250 r.p.m.) and diluted to an OD_{600} of 0.05 in fresh LB. A 10 μl volume of the sample was added to the wells with 90 μl of the diluted culture of reporter strain, and a 60 μl volume of filter-sterilized mineral oil was added in order to prevent evaporation during the assay. The *rhlA-lux* activities of the pDO100 strain were measured with a Synergy 2 Multi-Mode Microplate Reader, and calculated from the luminescence value minus that of the medium control. Each sample was tested in triplicate. CPS was normalized to OD_{600} of pDO100 (pKD-*rhlA*).

For preparation of the sample, an overnight culture of the tested strain in LB medium was washed and diluted 80-fold in 4 ml M8 minimal medium without antibiotics. The liquid culture was grown in a 20 ml tube at 37°C with shaking (250 r.p.m.). After incubation for 9 h (or the indicated time), 1 ml culture was centrifuged and sterilized by using a 0.22 μm pore size filter.

The bioassay of C4-HSL activity was also carried out using a tube culture method. In this assay, a 330 μl volume of sample was added to a 20 ml tube that contains 3 ml of the diluted culture of the reporter strain PDO100 (pKD-*rhlA*) as described above. The liquid culture was grown at 37°C with shaking (250 r.p.m.) and sampled at time points thereafter. Luminescence was measured at the indicated times with a Synergy 2 Multi-Mode Microplate Reader, and calculated from luminescence values minus that of the medium control. Each sample was tested in triplicate. CPS was normalized to OD_{600} of pDO100 (pKD-*rhlA*).

RNA-seq, data analyses and qRT-PCR

Overnight cultures in LB medium of the indicated strains were washed and diluted 80-fold in M8 minimal medium in a 20 ml tube with a flask volume-to-medium volume ratio of 5:1. The liquid culture was grown at 37°C for about 9 h with shaking (250 r.p.m.). Total RNA was immediately stabilized with RNAprotect Bacteria Reagent (Qiagen, Valencia, CA, USA) and then extracted by using a Qiagen RNeasy kit following the manufacturer's instructions. After rRNA was removed through the use of MICROBExpress Kit (Ambion), mRNA was used to generate the cDNA library according to the TruSeq RNA Sample Prep Kit protocol (Illumina), which was then sequenced using the HiSeq 2000 system (Illumina). Bacterial RNA-seq reads were mapped to the *P. aeruginosa* genomes, using TopHat (version 2.0.0) with two mismatches allowed (Trapnell *et al.*, 2009). Only uniquely mapped reads were kept for subsequent analyses. Two biological replicates were used for either the wild-type PAO1 or the Δ*crc* strain. The gene differential expression analysis was performed using Cuffdiff software (version 2.0.0) (Trapnell *et al.*, 2010). Criterion such as cutoff limitation for fold change ≥ 2 or ≤ 0.5 and Cuffdiff *P*-value < 0.05 was used to select differential expression genes.

For qRT-PCR analysis, the total DNase-treated RNA (5 μg) was reversely transcribed to synthesize cDNA using the PrimeScript RT reagent Kit (Takara) with random primers. Triplicate quantitative assays were performed on 1 μl of each cDNA dilution with the THUNDERBIRD™ SYBR® qPCR Mix (Toyobo) and 300 nM primers using an Applied Biosystems 7500 Fast Real-Time PCR System. Dissociation curve analysis was performed for verification of product homogeneity. The gene-specific primers used for qRT-PCR for *rhlA*, *rhlR*, *rhlI*, *lon*, *clpX*, *mmsa*, *rhlC* and *erbR* are listed in Supporting Information Table S2. The amplicon of 16S rRNA was used as an internal control. Relative expression levels of interest genes were calculated by the relative quantification method (ΔΔCT) as previously described (Livak and Schmittgen, 2001; Lan *et al.*, 2004; Cao *et al.*, 2014). As shown in Supporting Information Table S5, qRT-PCR confirmed all of the eight genes selected from the RNA-seq list, assuring the reliability and reproducibility of RNA-seq results.

In vivo degradation assays and Western blot analysis

The *in vivo* degradation assay was carried out in order to assess the stability of the RhlI-Flag protein in *P. aeruginosa* as previously described (Langklotz *et al*., 2011; Maisonneuve *et al*., 2013). Briefly, overnight LB cultures of tested strains were diluted 100-fold in fresh 20 ml LB medium in an Erlenmeyer flask with a flask volume-to-medium volume ratio of 5:1, and were aerated by shaking at 250 r.p.m. When the OD_{600} value of the culture reached approximately 0.5, chloramphenicol (a final concentration of 25 μg ml^{-1}) was added to the culture in order to block the translation, and samples for Western blot analysis were removed at the indicated times.

For the detection of either Lon-Flag or RhlI-Flag when bacteria were grown in M8 minimal medium, overnight LB cultures of the indicated strains were washed twice and diluted 80-fold in fresh M8 minimal medium. The liquid cultures were grown in a 20 ml tube with a tube volume-to-medium volume ratio of 5:1, shaking with 250 r.p.m. at 37°C for about 9 h. Equivalent OD_{600} units of cell cultures were harvested.

The samples were solubilized in the sodium dodecyl sulfate (SDS)-polyacrylamide gel electrophoresis (PAGE) loading buffer (50 mM Tris-HCl, pH 6.8; 2% SDS; 0.1% bromophenol blue; 1% mercaptoethanol; 10% glycerol) and then heated at 100°C for 15 min. SDS-PAGE was carried out according to the Laemmli method (Laemmli, 1970) using a 10% slab gel with a 5% stacking gel and transferred onto polyvinylidene fluoride (PVDF) (Bio-Rad) membranes. Subsequent incubation took place with a mouse anti-FLAG antibody (AOGMA, #AGM12165) or anti-RNAP antibody (Neoclone, #WP003), followed by a sheep anti-mouse immunoglobulin G antibody conjugated to horseradish peroxidase (GE Healthcare, #NA931) respectively. The membrane was exposed to X-ray film (Kodak) and alternatively the images were taken using Tanon-5200 Multi (Tanon, Shanghai, China), according to the manufacturer's recommendation. The relative abundance was determined by densitometric analysis using ImageQuant software (Molecular Dynamics, Sunnyvale, CA). Expression was normalized to RNA polymerase (RNAP) alpha subunit. Results are reported as fold changes with control bacteria set to 1, as indicated.

Construction, expression and purification of Lon-6His, 6His-Crc, 6His-Hfq and 6His-RhlI

For expression of Lon, pET22b (Novagen) was used as a vector. The *lon* gene was amplified using genomic DNA from *P. aeruginosa* PAO1 as a template with a pair of primers, Pro-lon-F and Pro-lon-R. The PCR primers were designed to allow in-frame fusion at the C-terminal end with the His tag from pET22b. The amplified fragment had an *Nde*I site at the 5′ end and *Hin*dIII site at the 3′ end. This fragment was digested with *Nde*I and *Hin*dIII and inserted into pET22b, digested with the same pair of the restriction enzymes to generate pET22b-Lon-6His.

Full-length of *crc*, *hfq* and *rhlI* were cloned into pET28a with a thrombin-cleavable N-terminal His-tag. Primer pairs Pro-crc-F/Pro-crc-R (*Bam*HI/*Hin*dIII), Pro-hfq-F/Pro-hfq-R (*Nde*I/*Xho*I) and Pro-rhlI-F/Pro-rhlI-R (*Nde*I/*Xho*I) were used to amplify the *crc*, *hfq* and *rhlI* genes from *P. aeruginosa* PAO1 chromosomal DNA respectively. The amplified fragments were ligated into similarly cut pET28a (Novagen) in order to produce the plasmids pET28a-6His-RhlI, pET28a-6His-Crc and pET28a-6His-Hfq.

The proteins were expressed in *E. coli* strain BL21 star (DE3) and purifications were performed as described in previous studies (Lan *et al*., 2010; Sun *et al*., 2012; Ding *et al*., 2014). Briefly, bacteria were grown at 37°C overnight in 10 ml of LB medium (containing 50 μg ml^{-1} kanamycin or 100 μg ml^{-1} carbenicillin) with shaking (250 r.p.m.). The next day, the cultures were transferred into 1 l of LB medium (containing 50 μg ml^{-1} kanamycin or 100 μg ml^{-1} carbenicillin) incubated at 37°C with shaking (250 r.p.m.) until the OD_{600} reached 0.6, and then IPTG (isopropyl-1-thio-β-d-galactopyranoside) was added to a final concentration of 1 mM. After overnight incubation at 16°C with shaking (250 r.p.m.), the cells were harvested by centrifugation. The cells were suspended in buffer A [20 mM Tris/HCl, pH 7.5; 200 mM NaCl, 1 mM dithiothreitol (DTT), 20 mM imidazole] and lysed at 4°C by sonication. Clarified cell lysate was loaded onto a HisTrap HP column (Amersham Biosciences), equilibrated with buffer A and eluted with a 0–100% gradient of buffer B (20 mM Tris/HCl, pH 7.5; 200 mM NaCl, 1 mM dithiothreitol (DTT), 500 mM imidazole). After that, the fractions containing either 6His-RhlI or 6His-Hfq were run on a desalting column, eluted with buffer A without imidazole, whereas 6His-Crc and Lon-6His proteins were further purified on a HiLoad 16/60 Superdex 75 prep grade and eluted with buffer A without imidazole. The purified protein was verified by SDS-PAGE followed by Coomassie blue staining. Protein concentrations were determined using the Pierce™ BCA Protein Assay Kit (Thermo, #23227).

Single reverse-phase liquid chromatography, mass spectrometry and database searching

Purified 6His-Crc protein sample was precipitated by mixing 1 volume of the cold sample solution with one-third volume of 100% (v/v) trichloroacetic acid (TCA) (6.1 N, Sigma) to give a final TCA concentration of 25%. Samples were left on ice for 3 h then centrifuged for 30 min at 4°C. The resulting pellets were washed twice with ice-cold acetone (500 ml each). After each wash, the solution was centrifuged for 10 min. Samples were air-dried.

Precipitated proteins were dissolved in 20 ml of 100 mM Tris-HCl, pH 8.5 containing 8M urea (Sigma). The protein was reduced by incubation in 5 mM tris(2-carboxyethyl)phosphine (TCEP) for 20 min at room temperature followed with carboxyamidomethylation of cysteines by incubation at room temperature for 30 min in the dark in 10 mM iodoacetamide. The sample was diluted fourfold (to 2 M of the concentration of urea) by the addition of an equal volume of 100 mM Tris-HCl, pH 8.5 and then trypsin (Promega) was added at a 1:20 enzyme to substrate ratio (wt:wt) and incubated at 37°C overnight in the dark. The resulting peptides from the digests were dissolved using 90% formic acid to a final concentration of 2% formic acid. The sample was stored at –20°C prior to liquid chromatography coupled with tandem mass spectrometry (LC-MS/MS) analysis.

The digested peptides (0.8 μg) were loaded on to an in-house packed reversed-phase C18 column (360 μm OD ×

100 μm ID) connected to an Agilent system. Peptides were analyzed by a 3 h gradient at a flow rate of 300 nl/min. The eluted peptides were ionized and introduced into a Thermo Scientific Q Exactive mass spectrometer using a nanospray source. A cycle of one full-scan MS spectrum (m/z 300–1800) was acquired followed by 20 MS/MS events, sequentially generated on the first to the 20th most intense ions selected from the full MS spectrum at a 27% normalized collision energy. The number of microscans was one for both MS and MS/MS scans and the maximum ion injection time was 50 ms and 100 ms respectively. MS scan functions and high-performance liquid chromatography (HPLC) solvent gradients were controlled by the Xcalibur data system (Thermo Fisher).

The acquired MS/MS were analyzed against a UniProtKB *E. coli* database and the protein sequence for *P. aeruginosa* Crc using Integrated Proteomics Pipeline (http://integratedproteomics.com/). The false discovery rate was set at 1% and precursor delta mass cutoff was 20 p.p.m. The mass of the amino acid cysteine was statically modified by +57.02146 Da in order to take into account the carboxyamidomethylation of the sample. Proteins identified are shown in Supporting Information Fig. S7. Normalized spectral abundance factor (NSAF) and exponentially modified protein abundance index (emPAI) calculated from all peptides identified are also presented and show the relative abundance of the protein Crc and Hfq, about 96% and 0.1% respectively (Supporting Information Fig. S7B) (Ishihama *et al.*, 2005; Zhang *et al.*, 2010; McIlwain *et al.*, 2012). The NSAF metric is defined as,

$$NSAF = \frac{s_N / L_N}{\sum_{i=1}^{n} (s_i / L_i)}$$

where N is the protein index, S_N is the number of spectra matched to protein N, L_N is the length of protein N and n is the total number of proteins in the input database.

RNA band-shift assays

For *in vitro* transcription of *lon* RNA, the PCR fragment (–215 to +236 of the start codon of *lon*) was generated with the primer pair lon-RNA-F/lon-RNA-R (Supporting Information Table S2) and was cloned into the pGEM-T Easy vector (Promega). The *lon* RNA was transcribed *in vitro* using Riboprobe® In Vitro Transcription Systems (Promega) according to the manufacturer's instructions, with pGEM-T/lon (Supporting Information Table S1) as a template. The mutant pGEM-T/lon-A456-GCC (Supporting Information Table S1) was obtained using QuikChange II site-directed mutagenesis kit (Stratagene) with primer pair A456-GCC-F/A456-GCC-R (Supporting Information Table S2).

The RNA was annealed by heating at 90°C for 9 min followed by slow cooling at room temperature for 30 min. A 80 nM annealed RNA was incubated with indicated amounts of either purified 6His-Crc or 6His-Hfq in 15 μl binding buffer A [10 mM Tris-Hcl, pH 7.5; 50 mM KCl, 5 mM $MgCl_2$, 10% (v/v) glycerol, 1 μg yeast tRNA and 20 U RNasin RNase inhibitor (Promega)]. The molar ratio between Hfq (expressed as monomers) and the *lon* RNA fragment ranges from 7.5 to 32.5, as indicated. After a 30 min incubation at room temperature, a 10 μl of the sample was loaded on a non-denaturing 4.5% polyacrylamide gel. Electrophoresis was performed at 4°C using 0.5 × TBE buffer (Tris-borate-ethylenediaminetetraacetic acid) (45 mM Tris-HCl, pH 8.3; 45 mM boric acid, 10 mM ethylenediaminetetraacetic acid) as running buffer at 90 V for 100 min. The gel was stained with GelRed nucleic acid staining solution (Biotium) for 5 min and the images were taken using Tanon-5200 Multi as described previously (Cao *et al.*, 2014; Ding *et al.*, 2014).

Dye primer-based RNase ONE footprinting assays

The published RNase-based footprinting protocol (Peng *et al.*, 2012) and dye primer-based footprinting protocol (Zianni *et al.*, 2006; Cao *et al.*, 2014; Ding *et al.*, 2014) were modified. Briefly, the *lon* mRNA (*lon*$_{-215\ \text{to}\ +236}$) was annealed by heating at 90°C for 9 min followed by slow cooling at room temperature for 30 min. After that, 120 nM annealed RNA was incubated in a 55 μl binding buffer (10 mM Tris-HCl, pH 7.5; 50 mM KCl; 5 mM $MgCl_2$) supplied with or without 6His-Hfq (12 μM). After a 30 min incubation at room temperature, 8 μl RNase ONE (0.025 U μl^{-1}, Promega, #M4261) was added to the reaction mixture and incubated for three more minutes. The reactions were quenched by adding phenol and vortexing vigorously (Peng *et al.*, 2012). The mixture was extracted with phenol-chloroform-isoamyl alcohol (25:24:1) (Peng *et al.*, 2012). The digested RNA fragments were isolated by ethanol precipitation, dried under vacuum and resuspended in RNase-free water.

The primer extension reaction was performed by using PrimeScript RT Enzyme Mix (Takara, #RR037A), digested RNA and 6-carboxyfluorescein (6-FAM)-labeled primer lon-RNA-FAM (Supporting Information Table S2) according to the manufacturer's recommendation. The cDNA fragments were isolated by ethanol precipitation, and mixed with 4.9 μl of HiDi formamide and 0.1 μl of GeneScan-500 LIZ size standards (Applied Biosystems). A 3730xl DNA analyzer was used to detect the sample, and the result was analyzed with GeneMapper software (Applied Biosystems). The dye primer-based sequencing kit (Thermo, #79260) was used in order to more precisely determine the sequences after the capillary electrophoresis results of the reactions were aligned, and pGEM-T/lon plasmid DNA was used as template for DNA sequencing. Electropherograms were then analyzed with GeneMarker v1.8 (Applied Biosystems).

In vitro *proteolysis of RhlI*

The *in vitro* proteolysis of RhlI was performed as previously described (Herbst *et al.*, 2009) with some modifications. A concentration of 10 μM 6His-RhlI was mixed with 4 μM Lon-6His in a reaction buffer containing 50 mM Tris-HCl (pH 8.0), 10 mM $MgCl_2$, 1 mM DTT, 50 mM creatine phosphate (Sigma, #27920), 80 μg ml^{-1} creatine phosphokinase (Sigma, #C3755) and 4 mM ATP. Reaction mixture was incubated at 37°C and a 15 μl aliquot was removed at the indicated time. The reaction was stopped by adding SDS-PAGE loading buffer and heated at 100°C for 15 min. Degradation of 6His-RhlI was subsequently visualized by 10% SDS-PAGE and Coomassie staining. Images were taken using Tanon-5200 Multi.

Lettuce leaf model of infection

A lettuce leaf virulence assay was performed as described previously (Rahme *et al.*, 1997; Filiatrault *et al.*, 2006;

Goldova *et al.*, 2011; Cao *et al.*, 2014). Briefly, *P. aeruginosa* strains were grown aerobically overnight at 37°C with shaking (250 r.p.m.) in LB medium, washed, resuspended and diluted in sterile $MgSO_4$ to a bacterial density of 1×10^9 CFU/ml. Lettuce leaves were prepared by washing with sterile distilled H_2O and 0.1% bleach. Samples (10 μl) were then inoculated into the midribs of romaine lettuce leaves. Containers of Whatman paper moistened with 10 mM MgSO4 and inoculated leaves were kept in a growth chamber at 37°C for 5 days. Symptoms were monitored daily.

Mouse model of acute pneumonia

Mouse infections were carried out as previously described (Lan *et al.*, 2010; Cao *et al.*, 2014) with some modifications, using 8-week-old female C57BL/6 mice obtained from Shanghai SLAC Laboratory Animal and housed under specified pathogen-free conditions. All animal experiments were reviewed and approved by the Institutional Animal Care and Use Committee of Shanghai Public Health Clinical Center and were performed in accordance with relevant guidelines and regulations. Mice were anaesthetized with pentobarbital sodium (intraperitoneal injection, 80 mg kg^{-1}) and intranasally infected with c. 5×10^6 CFU of each bacterial isolate; the actual inoculum titer for each group was determined by plating serial dilutions. Animals were sacrificed 18 h post-infection. Lungs were aseptically removed and homogenized in phosphate-buffered saline plus 0.1% Triton X-100 to obtain single-cell suspensions. Serial dilutions of each organ were plated on PIA (Difco) plates. Bacterial burden per organ was calculated and is expressed as a ratio of the inoculum delivered per animal. Statistical analysis was performed using Prism software (GraphPad).

Acknowledgements

We would like to thank Professor H.P. Schweizer (Colorado State University) for kindly providing us plasmids pEX18Ap and pPS858, Professor Haihua Liang (Northwest University, China) for providing us plasmids pMS402 and pDO100 (pKD-*rhlA*) strain, and Professor Matthew Parsek (University of Washington) for providing us plasmid mini-CTX-lacZ-EB. We thank S.F. Reichard, M.A. for editing the manuscript. This work was financially supported by National Natural Science Foundation of China grants (31270126), Shanghai Committee of Science and Technology grants (12JC1410200), the National Science and Technology Major Project 'Key New Drug Creation and Manufacturing Program' (2014ZX09507009-015) and the Hundred Talents Program of the Chinese Academy of Sciences (to L.L.).

Conflict of interest

The authors declare no conflict of interest.

References

Balasubramanian, D., Schneper, L., Kumari, H., and Mathee, K. (2013) A dynamic and intricate regulatory network determines *Pseudomonas aeruginosa* virulence. *Nucleic Acids Res* **41:** 1–20.

Becher, A., and Schweizer, H.P. (2000) Integration-proficient *Pseudomonas aeruginosa* vectors for isolation of single-copy chromosomal lacZ and lux gene fusions. *Biotechniques* **29:** 948–950, 952.

Brazas, M.D., Breidenstein, E.B., Overhage, J., and Hancock, R.E. (2007) Role of lon, an ATP-dependent protease homolog, in resistance of *Pseudomonas aeruginosa* to ciprofloxacin. *Antimicrob Agents Chemother* **51:** 4276–4283.

Breidenstein, E.B., Janot, L., Strehmel, J., Fernandez, L., Taylor, P.K., Kukavica-Ibrulj, I., *et al.* (2012) The Lon protease is essential for full virulence in *Pseudomonas aeruginosa*. *PLoS ONE* **7:** e49123.

Brint, J.M., and Ohman, D.E. (1995) Synthesis of multiple exoproducts in *Pseudomonas aeruginosa* is under the control of RhlR-RhlI, another set of regulators in strain PAO1 with homology to the autoinducer-responsive LuxR-LuxI family. *J Bacteriol* **177:** 7155–7163.

Caiazza, N.C., Shanks, R.M., and O'Toole, G.A. (2005) Rhamnolipids modulate swarming motility patterns of *Pseudomonas aeruginosa*. *J Bacteriol* **187:** 7351–7361.

Cao, Q., Wang, Y., Chen, F., Xia, Y., Lou, J., Zhang, X., *et al.* (2014) A Novel signal transduction pathway that modulates rhl quorum sensing and bacterial virulence in *Pseudomonas aeruginosa*. *PLoS Pathog* **10:** e1004340.

Choi, K.H., Kumar, A., and Schweizer, H.P. (2006) A 10-min method for preparation of highly electrocompetent *Pseudomonas aeruginosa* cells: application for DNA fragment transfer between chromosomes and plasmid transformation. *J Microbiol Methods* **64:** 391–397.

Croda-Garcia, G., Grosso-Becerra, V., Gonzalez-Valdez, A., Servin-Gonzalez, L., and Soberon-Chavez, G. (2011) Transcriptional regulation of *Pseudomonas aeruginosa* rhlR: role of the CRP orthologue Vfr (virulence factor regulator) and quorum-sensing regulators LasR and RhlR. *Microbiology* **157:** 2545–2555.

Dandekar, A.A., and Greenberg, E.P. (2013) Microbiology: plan B for quorum sensing. *Nat Chem Biol* **9:** 292–293.

Deng, X., Sun, F., Ji, Q., Liang, H., Missiakas, D., Lan, L., and He, C. (2012) Expression of multidrug resistance efflux pump gene norA is iron responsive in *Staphylococcus aureus*. *J Bacteriol* **194:** 1753–1762.

Ding, Y., Liu, X., Chen, F., Di, H., Xu, B., Zhou, L., *et al.* (2014) Metabolic sensor governing bacterial virulence in *Staphylococcus aureus*. *Proc Natl Acad Sci USA* **111:** E4981–E4990.

Duan, K., Dammel, C., Stein, J., Rabin, H., and Surette, M.G. (2003) Modulation of *Pseudomonas aeruginosa* gene expression by host microflora through interspecies communication. *Mol Microbiol* **50:** 1477–1491.

Filiatrault, M.J., Picardo, K.F., Ngai, H., Passador, L., and Iglewski, B.H. (2006) Identification of *Pseudomonas aeruginosa* genes involved in virulence and anaerobic growth. *Infect Immun* **74:** 4237–4245.

Goldova, J., Ulrych, A., Hercik, K., and Branny, P. (2011) A eukaryotic-type signalling system of *Pseudomonas aeruginosa* contributes to oxidative stress resistance, intracellular survival and virulence. *BMC Genomics* **12:** 437.

Gorke, B., and Stulke, J. (2008) Carbon catabolite repression in bacteria: many ways to make the most out of nutrients. *Nat Rev Microbiol* **6:** 613–624.

Gottesman, S. (1996) Proteases and their targets in *Escherichia coli*. *Annu Rev Genet* **30:** 465–506.

Gottesman, S., Wickner, S., and Maurizi, M.R. (1997) Protein quality control: triage by chaperones and proteases. *Genes Dev* **11:** 815–823.

Gupta, R., Gobble, T.R., and Schuster, M. (2009) GidA posttranscriptionally regulates rhl quorum sensing in *Pseudomonas aeruginosa*. *J Bacteriol* **191:** 5785–5792.

Herbst, K., Bujara, M., Heroven, A.K., Opitz, W., Weichert, M., Zimmermann, A., and Dersch, P. (2009) Intrinsic thermal sensing controls proteolysis of *Yersinia* virulence regulator RovA. *PLoS Pathog* **5:** e1000435.

Hoang, T.T., Karkhoff-Schweizer, R.R., Kutchma, A.J., and Schweizer, H.P. (1998) A broad-host-range Flp-FRT recombination system for site-specific excision of chromosomally-located DNA sequences: application for isolation of unmarked *Pseudomonas aeruginosa* mutants. *Gene* **212:** 77–86.

Irie, Y., Starkey, M., Edwards, A.N., Wozniak, D.J., Romeo, T., and Parsek, M.R. (2010) *Pseudomonas aeruginosa* biofilm matrix polysaccharide Psl is regulated transcriptionally by RpoS and post-transcriptionally by RsmA. *Mol Microbiol* **78:** 158–172.

Ishihama, Y., Oda, Y., Tabata, T., Sato, T., Nagasu, T., Rappsilber, J., and Mann, M. (2005) Exponentially modified protein abundance index (emPAI) for estimation of absolute protein amount in proteomics by the number of sequenced peptides per protein. *Mol Cell Proteomics* **4:** 1265–1272.

Jansons, I., Touchie, G., Sharp, R., Almquist, K., Farinha, M.A., Lam, J.S., and Kropinski, A.M. (1994) Deletion and transposon mutagenesis and sequence analysis of the pRO1600 OriR region found in the broad-host-range plasmids of the pQF series. *Plasmid* **31:** 265–274.

Jensen, P.O., Bjarnsholt, T., Phipps, R., Rasmussen, T.B., Calum, H., Christoffersen, L., *et al*. (2007) Rapid necrotic killing of polymorphonuclear leukocytes is caused by quorum-sensing-controlled production of rhamnolipid by *Pseudomonas aeruginosa*. *Microbiology* **153:** 1329–1338.

Jimenez, P.N., Koch, G., Thompson, J.A., Xavier, K.B., Cool, R.H., and Quax, W.J. (2012) The multiple signaling systems regulating virulence in *Pseudomonas aeruginosa*. *Microbiol Mol Biol Rev* **76:** 46–65.

Kohler, T., Curty, L.K., Barja, F., van Delden, C., and Pechere, J.C. (2000) Swarming of *Pseudomonas aeruginosa* is dependent on cell-to-cell signaling and requires flagella and pili. *J Bacteriol* **182:** 5990–5996.

Kohler, T., Guanella, R., Carlet, J., and van Delden, C. (2010) Quorum sensing-dependent virulence during *Pseudomonas aeruginosa* colonisation and pneumonia in mechanically ventilated patients. *Thorax* **65:** 703–710.

Kulasekara, H.D., Ventre, I., Kulasekara, B.R., Lazdunski, A., Filloux, A., and Lory, S. (2005) A novel two-component system controls the expression of *Pseudomonas aeruginosa* fimbrial cup genes. *Mol Microbiol* **55:** 368–380.

Laemmli, U.K. (1970) Cleavage of structural proteins during the assembly of the head of bacteriophage T4. *Nature* **227:** 680–685.

Lan, L., Chen, W., Lai, Y., Suo, J., Kong, Z., Li, C., *et al*. (2004) Monitoring of gene expression profiles and isolation of candidate genes involved in pollination and fertilization in rice (*Oryza sativa* L.) with a 10K cDNA microarray. *Plant Mol Biol* **54:** 471–487.

Lan, L., Murray, T.S., Kazmierczak, B.I., and He, C. (2010) *Pseudomonas aeruginosa* OspR is an oxidative stress sensing regulator that affects pigment production, antibiotic resistance and dissemination during infection. *Mol Microbiol* **75:** 76–91.

Langklotz, S., Schakermann, M., and Narberhaus, F. (2011) Control of lipopolysaccharide biosynthesis by FtsH-mediated proteolysis of LpxC is conserved in enterobacteria but not in all gram-negative bacteria. *J Bacteriol* **193:** 1090–1097.

Liang, H., Duan, J., Sibley, C.D., Surette, M.G., and Duan, K. (2011) Identification of mutants with altered phenazine production in *Pseudomonas aeruginosa*. *J Med Microbiol* **60:** 22–34.

Liang, H., Deng, X., Ji, Q., Sun, F., Shen, T., and He, C. (2012) The *Pseudomonas aeruginosa* global regulator VqsR directly inhibits QscR to control quorum-sensing and virulence gene expression. *J Bacteriol* **194:** 3098–3108.

Linares, J.F., Moreno, R., Fajardo, A., Martinez-Solano, L., Escalante, R., Rojo, F., and Martinez, J.L. (2010) The global regulator Crc modulates metabolism, susceptibility to antibiotics and virulence in *Pseudomonas aeruginosa*. *Environ Microbiol* **12:** 3196–3212.

Livak, K.J., and Schmittgen, T.D. (2001) Analysis of relative gene expression data using real-time quantitative PCR and the 2(-Delta Delta C(T) Method. *Methods* **25:** 402–408.

Lyczak, J.B., Cannon, C.L., and Pier, G.B. (2002) Lung infections associated with cystic fibrosis. *Clin Microbiol Rev* **15:** 194–222.

McClure, C.D., and Schiller, N.L. (1996) Inhibition of macrophage phagocytosis by *Pseudomonas aeruginosa* rhamnolipids in vitro and in vivo. *Curr Microbiol* **33:** 109–117.

McIlwain, S., Mathews, M., Bereman, M.S., Rubel, E.W., MacCoss, M.J., and Noble, W.S. (2012) Estimating relative abundances of proteins from shotgun proteomics data. *BMC Bioinformatics* **13:** 308.

Madhushani, A., Del Peso-Santos, T., Moreno, R., Rojo, F., and Shingler, V. (2014) Transcriptional and translational control through the 5′-leader region of the dmpR master regulatory gene of phenol metabolism. *Environ Microbiol* **17:** 119–133.

Maisonneuve, E., Castro-Camargo, M., and Gerdes, K. (2013) p)ppGpp controls bacterial persistence by stochastic induction of toxin-antitoxin activity. *Cell* **154:** 1140–1150.

Marr, A.K., Overhage, J., Bains, M., and Hancock, R.E. (2007) The Lon protease of *Pseudomonas aeruginosa* is induced by aminoglycosides and is involved in biofilm formation and motility. *Microbiology* **153:** 474–482.

Maurizi, M.R. (1992) Proteases and protein degradation in *Escherichia coli*. *Experientia* **48:** 178–201.

Milojevic, T., Grishkovskaya, I., Sonnleitner, E., Djinovic-Carugo, K., and Blasi, U. (2013) The *Pseudomonas aeruginosa* catabolite repression control protein Crc is devoid of RNA binding activity. *PLoS ONE* **8:** e64609.

Moreno, R., Hernandez-Arranz, S., La Rosa, R., Yuste, L., Madhushani, A., Shingler, V., and Rojo, F. (2014) The Crc and Hfq proteins of *Pseudomonas* putida cooperate in catabolite repression and formation of ribonucleic acid complexes with specific target motifs. *Environ Microbiol* **17:** 105–118.

National Nosocomial Infections Surveillance (2004) National Nosocomial Infections Surveillance (NNIS) system report, data summary from January 1992 through June 2004, issued October 2004. *Am J Infect Control* **32:** 470–485.

Ochsner, U.A., and Reiser, J. (1995) Autoinducer-mediated regulation of rhamnolipid biosurfactant synthesis in *Pseudomonas aeruginosa*. *Proc Natl Acad Sci USA* **92:** 6424–6428.

Ochsner, U.A., Fiechter, A., and Reiser, J. (1994) Isolation, characterization, and expression in *Escherichia coli* of the *Pseudomonas aeruginosa* rhlAB genes encoding a rhamnosyltransferase involved in rhamnolipid biosurfactant synthesis. *J Biol Chem* **269:** 19787–19795.

O'Loughlin, C.T., Miller, L.C., Siryaporn, A., Drescher, K., Semmelhack, M.F., and Bassler, B.L. (2013) A quorum-sensing inhibitor blocks *Pseudomonas aeruginosa* virulence and biofilm formation. *Proc Natl Acad Sci USA* **110:** 17981–17986.

Peng, Y., Soper, T.J., and Woodson, S.A. (2012) RNase footprinting of protein binding sites on an mRNA target of small RNAs. *Methods Mol Biol* **905:** 213–224.

Qiu, D., Eisinger, V.M., Head, N.E., Pier, G.B., and Yu, H.D. (2008) ClpXP proteases positively regulate alginate overexpression and mucoid conversion in *Pseudomonas aeruginosa*. *Microbiology* **154:** 2119–2130.

Rabinowitz, J.D., and Silhavy, T.J. (2013) Systems biology: metabolite turns master regulator. *Nature* **500:** 283–284.

Rahim, R., Ochsner, U.A., Olvera, C., Graninger, M., Messner, P., Lam, J.S., and Soberon-Chavez, G. (2001) Cloning and functional characterization of the *Pseudomonas aeruginosa* rhlC gene that encodes rhamnosyltransferase 2, an enzyme responsible for di-rhamnolipid biosynthesis. *Mol Microbiol* **40:** 708–718.

Rahme, L.G., Tan, M.W., Le, L., Wong, S.M., Tompkins, R.G., Calderwood, S.B., and Ausubel, F.M. (1997) Use of model plant hosts to identify *Pseudomonas aeruginosa* virulence factors. *Proc Natl Acad Sci USA* **94:** 13245–13250.

Reis, R.S., Pereira, A.G., Neves, B.C., and Freire, D.M. (2011) Gene regulation of rhamnolipid production in *Pseudomonas aeruginosa* – a review. *Bioresour Technol* **102:** 6377–6384.

Rojo, F. (2010) Carbon catabolite repression in *Pseudomonas*: optimizing metabolic versatility and interactions with the environment. *FEMS Microbiol Rev* **34:** 658–684.

Rumbaugh, K.P., Griswold, J.A., Iglewski, B.H., and Hamood, A.N. (1999) Contribution of quorum sensing to the virulence of *Pseudomonas aeruginosa* in burn wound infections. *Infect Immun* **67:** 5854–5862.

Rutherford, S.T., and Bassler, B.L. (2012) Bacterial quorum sensing: its role in virulence and possibilities for its control. *Cold Spring Harb Perspect Med* **2:** a012427.

Schuster, M., and Greenberg, E.P. (2006) A network of networks: quorum-sensing gene regulation in *Pseudomonas aeruginosa*. *Int J Med Microbiol* **296:** 73–81.

Smith, R.S., and Iglewski, B.H. (2003) *P. aeruginosa* quorum-sensing systems and virulence. *Curr Opin Microbiol* **6:** 56–60.

Sonnleitner, E., and Blasi, U. (2014) Regulation of Hfq by the RNA CrcZ in *Pseudomonas aeruginosa* carbon catabolite repression. *PLoS Genet* **10:** e1004440.

Sonnleitner, E., Hagens, S., Rosenau, F., Wilhelm, S., Habel, A., Jager, K.E., and Blasi, U. (2003) Reduced virulence of a hfq mutant of *Pseudomonas aeruginosa* O1. *Microb Pathog* **35:** 217–228.

Sonnleitner, E., Schuster, M., Sorger-Domenigg, T., Greenberg, E.P., and Blasi, U. (2006) Hfq-dependent alterations of the transcriptome profile and effects on quorum sensing in *Pseudomonas aeruginosa*. *Mol Microbiol* **59:** 1542–1558.

Sonnleitner, E., Abdou, L., and Haas, D. (2009) Small RNA as global regulator of carbon catabolite repression in *Pseudomonas aeruginosa*. *Proc Natl Acad Sci USA* **106:** 21866–21871.

Sorger-Domenigg, T., Sonnleitner, E., Kaberdin, V.R., and Blasi, U. (2007) Distinct and overlapping binding sites of *Pseudomonas aeruginosa* Hfq and RsmA proteins on the non-coding RNA RsmY. *Biochem Biophys Res Commun* **352:** 769–773.

Stover, C.K., Pham, X.Q., Erwin, A.L., Mizoguchi, S.D., Warrener, P., Hickey, M.J., *et al*. (2000) Complete genome sequence of *Pseudomonas aeruginosa* PAO1, an opportunistic pathogen. *Nature* **406:** 959–964.

Sun, F., Ding, Y., Ji, Q., Liang, Z., Deng, X., Wong, C.C., *et al*. (2012) Protein cysteine phosphorylation of SarA/MgrA family transcriptional regulators mediates bacterial virulence and antibiotic resistance. *Proc Natl Acad Sci USA* **109:** 15461–15466.

Takaya, A., Tabuchi, F., Tsuchiya, H., Isogai, E., and Yamamoto, T. (2008) Negative regulation of quorum-sensing systems in *Pseudomonas aeruginosa* by ATP-dependent Lon protease. *J Bacteriol* **190:** 4181–4188.

Trapnell, C., Pachter, L., and Salzberg, S.L. (2009) TopHat: discovering splice junctions with RNA-Seq. *Bioinformatics* **25:** 1105–1111.

Trapnell, C., Williams, B.A., Pertea, G., Mortazavi, A., Kwan, G., van Baren, M.J., *et al*. (2010) Transcript assembly and quantification by RNA-Seq reveals unannotated transcripts and isoform switching during cell differentiation. *Nat Biotechnol* **28:** 511–515.

Vogel, J., and Luisi, B.F. (2011) Hfq and its constellation of RNA. *Nat Rev Microbiol* **9:** 578–589.

Wenner, N., Maes, A., Cotado-Sampayo, M., and Lapouge, K. (2013) NrsZ: a novel, processed, nitrogen-dependent, small non-coding RNA that regulates *Pseudomonas aeruginosa* PAO1 virulence. *Environ Microbiol* **16:** 1053–1068.

Whiteley, M., Parsek, M.R., and Greenberg, E.P. (2000) Regulation of quorum sensing by RpoS in *Pseudomonas aeruginosa*. *J Bacteriol* **182:** 4356–4360.

Wickner, S., Maurizi, M.R., and Gottesman, S. (1999) Post-translational quality control: folding, refolding, and degrading proteins. *Science* **286:** 1888–1893.

Williams, P., and Camara, M. (2009) Quorum sensing and environmental adaptation in *Pseudomonas aeruginosa*: a tale of regulatory networks and multifunctional signal molecules. *Curr Opin Microbiol* **12:** 182–191.

Zhang, L., Gao, Q., Chen, W., Qin, H., Hengzhuang, W., Chen, Y., *et al*. (2013) Regulation of pqs quorum sensing via catabolite repression control in *Pseudomonas aeruginosa*. *Microbiology* **159:** 1931–1936.

Zhang, Y., Wen, Z., Washburn, M.P., and Florens, L. (2010) Refinements to label free proteome quantitation: how to deal with peptides shared by multiple proteins. *Anal Chem* **82:** 2272–2281.

Zhu, H., Bandara, R., Conibear, T.C., Thuruthyil, S.J., Rice, S.A., Kjelleberg, S., *et al*. (2004) *Pseudomonas aeruginosa* with lasI quorum-sensing deficiency during corneal infection. *Invest Ophthal Vis Sci* **45:** 1897–1903.

Zianni, M., Tessanne, K., Merighi, M., Laguna, R., and Tabita, F.R. (2006) Identification of the DNA bases of a DNase I footprint by the use of dye primer sequencing on an automated capillary DNA analysis instrument. *J Biomol Tech* **17:** 103–113.

Zulianello, L., Canard, C., Kohler, T., Caille, D., Lacroix, J.S., and Meda, P. (2006) Rhamnolipids are virulence factors that promote early infiltration of primary human airway epithelia by *Pseudomonas aeruginosa*. *Infect Immun* **74:** 3134–3147.

Supporting information

Additional supporting information may be found in the online version of this article at the publisher's web-site.